MASTER'S THESIS - TATIANNA WAI YING WONG

ESSENTIAL RESIDUES IN IMC RECRUITMENT OF *PF*GAP45 IN THE MALARIA PARASITE

By TATIANNA WAI YING WONG, B.Sc.

A Thesis Submitted to the School of Graduate Studies in Partial Fulfillment of the

Requirements for the Degree Master of Science

Table of Contents

I. Descriptive Note

MASTER OF SCIENCE (2015) McMaster University, Hamilton, Ontario

TITLE: Essential residues in IMC recruitment of *Pf*GAP45 in the malaria parasite

AUTHOR: Tatianna Wai Ying Wong

SUPERVISOR: Dr. Tim Gilberger

NUMBER OF PAGES: xii, 70

II. Abstract

The *Plasmodium falciparum* merozoite utilizes an actin-myosin motor to invade into erythrocytes, which is a part of the protein complex termed the glideosome. The glideosome provides the parasite with substrate dependent gliding motility, and is connected to the unique organelle named the **i**nner **m**embrane **c**omplex (IMC). The **g**lideosome **a**ssociated **p**rotein 45 (GAP45) is a crucial member of the glideosome. Here, we investigate the differential role of two post-translational modifications, specifically palmitoylation and phosphorylation, for recruitment of the protein to the IMC as well as glideosome association. Through comprehensive mutational analysis, it was shown that in addition to the N-terminal dual acylation motif, the C-terminal residues C189 and C192 must be present to mediate GAP45 recruitment to the IMC. Despite the abundant *in vivo* phosphorylation sites in GAP45, a phosphorylation null mutant does not affect the protein's IMC localization. Therefore this modification may be involved in glideosome complex formation, which will be further investigated through co-immunoprecipitation and gaining structural insight of GAP45.

III. Acknowledgements

For the past two years, I have a lot of people I would like to thank for their mentorship and support. Starting off with my McMaster lab members Johanna, Dhaneswar, Josh, and Olivia. Thank you to Johanna for the training, Dhaneswar for the mentorship about life, and Josh and Olivia for just being awesome people. Also at McMaster are Sharon, Austin, and Derek, my fellow nerds who I had lunch dates/coffee/Skype with to keep each other mentally in check.

In Germany I have absolutely too many people to thank. Here I am going to start off with my lovely flatmate Palmmii. Thank you for feeding me with insanely amazing Thai food (especially that fried fish and the curry YUM), and making sure that I am eating at all time. I will miss our shopping trips and our long girl chats. You have really made me feel like Hamburg was home. Also a shout out to Fabian, who somehow became our father/girlfriend, and all the amazing people I met in Hamburg. You guys made it more than I ever thought it would have been.

Then I would like to thank my lab mates in Germany, Misses Maya, Louisa, Dorothee, Ann-Ka, Bärbel, Alex, Leonie, Maria, Viola, and Melissa, and of course the Misters Sven, Ferdi, Jakob, Paolo, Flo, and Ernst. Also a big shout out to Nicci! You guys have made Hamburg incredible for me. Thank you guys for showing me what Hamburg is all about. I will miss those long work nights very very much. We are very hardworking people. I can't really thank each of you individually or else I may end up exceeding page limit, but I will always remember you guys.

And obviously thank you to my parents. They were very supportive of me going overseas, and even came to visit me in Europe. They often questioned whether I was alive with many many cap locked emails, but I am still up and running, and back in the homeland. Also a big thank you to my brother and Michelle for coming to visit me in Hamburg. Unfortunately I wasn't able to take them around so much as I was quite new myself, but I'm so happy they came when I was the most homesick.

I would like to thank my dear friends at home as well. Thank you to Peter Mi for being my punching bag (not literally), Alissa for sneaking out during lunch breaks to Skype with me, my international expat girlfriends Mel and Co for those desperately hilarious WhatsApp conversations to keep us all sane, Jenny and Wendy for their bubbliness, Daria's wisdom for keeping me grounded, and Gary and Evelyn for always keeping an open ear for me.

Also thank you to my committee members Dr. Bowdish and Dr. Wright for their support and mentorship. I would also like to thank Dr. Tobias Spielmann for his wisdom and calmness when dealing with the scrambling me when I am trying to find digitonin, antibodies and a scanner.

And finally, I would like give a ginormous thanks my supervisor and mentor, Tim. From looking at my failed gels and PCRs back in my third year of undergrad to giving me this

opportunity to be in Hamburg, Germany, thank you. You have given so many opportunities and helped me grow so much as a student and as a scientist.

IV. List of Figures and Tables

List of Figures

List of Tables

V. List of Abbreviations and Symbols

Abbreviation	
ABE	Acyl-biotin exchange
ama1	Apical membrane antigen 1
AMP	Adenosine monophosphate
APT	Acyl-protein thioesterase
ARO	Armadillo repeats-only protein
ATP	Adenosine triphosphate
bp	Base pairs
BSA	Bovine serum albumin
CaMK	Calcium/calmodulin-dependent protein kinase
CDPK	Calcium dependent protein kinase
CK1	Casein kinase 1
CRT	Chloroquine resistance transporter
Da	daltons
DAPI	4',6-diamidino-2-phenylindole
DBL	Duffy binding-like ligands
DDT	Dichlorodiphenyltrichloroethane
DMSO	Dimethyl sulfoxide
DNA	Deoxyribonucleic acid
dNTPs	Deoxynucleotides
EDTA	Ethylenediamine tetraacetic acid
EGTA	Ethylene glycol tetraacetic acid
EM	Electron microscopy
ER	Endoplasmic reticulum

EtOH	Ethanol
F	Filamentous
FPLC	Fast protein liquid chromotography
GAP	Glideosome associated protein
GFP	Green fluorescent protein
hdhfr	Human dihydrofolate reductase
hpi	Hours post invasion
ICAM	Intercellular adhesion molecule
IFA	Immunofluorescence assay
IPTG	Isopropyl-beta-D-thiogalactopyranoside
IMC	Inner membrane complex
iRBC	Infected red blood cells
IRS	Indoor residual spraying
ISP	IMC sub-compartment protein
ITN	Insecticide-treated net
kDa	Kilodaltons
l	Liter
LB	Lysogeny broth
µL	Microliter
µM	Micromolar
MDR	Multidrug resistance
Min	Minute(s)
mL	Milliliter
MLCC	Metabolic labeling/click chemistry
mm	Millimeter

mM	Millimolar
MSP	Merozoite surface protein
MWCO	Molecular weight cut-off
NMT	N-Myristoyltransferase
OD	Optical density
PAT	Palmitoyl-acyl transferase
PBS	Phosphate buffered saline
PCR	Polymerase chain reaction
pH	Potential Hydrogenii
pI	Isoelectric point
PI	Protease inhibitor
PKA	Protein kinase A
PKB	Protein kinase B
POP	Persistant organic pollutant
PPM	Parasite plasma membrane
psi	Pounds per square inch
PVM	Parasitophorous vacuole membrane
RBC	Red blood cell
RFP	Red fluorescent protein
RH	Reticulocyte homology
RON	Rhoptry neck protein
rpm	Revolutions per minute
SDS	Sodium dodecyl sulfate
SDS-PAGE	Sodium dodecyl sulfate polyacrylamide gel electrophoresis
Sec	Second(s)

SoTE	Sorbitol Tris-EDTA buffer
TCA	Trichloroacetic acid
TCEP	Tris(2-carboxyethyl)phosphine hydrochloride
TE	Tris-EDTA buffer
TEMED	N, N, N', N'-Tetramethylethylenediamine
TFB	Transformation buffer
U	units
V	Volt
v/v	Volume concentration
w/v	Mass concentration
WHO	World Health Organization

VI. Declaration of Academic Achievement

The constructs $GAP45_{phosnull}$-mCherry and $_{\Delta 29}$GAP45-mCherry were cloned by Tatianna and transfected by Dhaneswar Prusty. Live cell microscopy and Western blots for all cell lines except for $GAP45_{C160A}$-mCherry were completed by Tatianna. Proteinase K protection assay was also conducted by Tatianna. Protein purification at the DESY campus in Hamburg, Germany was conducted by Tatianna in collaboration with the Löw group.

The cloning and transfection for the wild type GAP45, $GAP45_{C160A}$, $GAP45_{C176AC178A}$, $GAP45_{C178A}$, $GAP45_{C189A}$, $GAP45_{C192A}$, and $GAP45_{palmnull}$ constructs were conducted by Olivia Ramsay. The Western blot for the $GAP45_{C160A}$-mCherry was also completed by Olivia Ramsay.

GAP50-GFP and GAP40-GFP overexpressing cell lines were generated and provided by Dr. Maya Kono.

1. Introduction

1.1 Epidemiology of malaria

Malaria is an infectious disease affecting subtropical and tropical regions in Africa, India, Southeast Asia, and South America (Figure 1). The disease is caused by parasites of the genus *Plasmodium* spp., causing 1.24 million deaths in 2010 (Murray et al., 2012). The disease mainly affects pregnant women, young children, and individuals with HIV (Shetty et al., 2012).

Within the genus *Plasmodium* spp., only five species are pathogenic towards humans, namely *P. vivax*, *P. malariae*, *P. ovale*, *P. knowlesi*, and *P. falciparum* (Kalanon & McFadden, 2010). Among the five species, *P. falciparum* causes the most lethal form of malaria (Vulliez-Le Normand et al., 2012). The parasite is transmitted to the human host by a female *Anopheles* mosquito via a blood meal. In the human host, the parasite eventually invades red blood cells as part of the intraerythrocytic cycle (refer to Section 1.3). This part of the parasite life cycle is responsible for all clinical symptoms associated with malaria. Some symptoms associated with falciparum malaria include fever, acute renal failure, severe anemia, metabolic acidosis, cerebral malaria, and coma, which may lead to death if not properly treated (Waller et al., 1995).

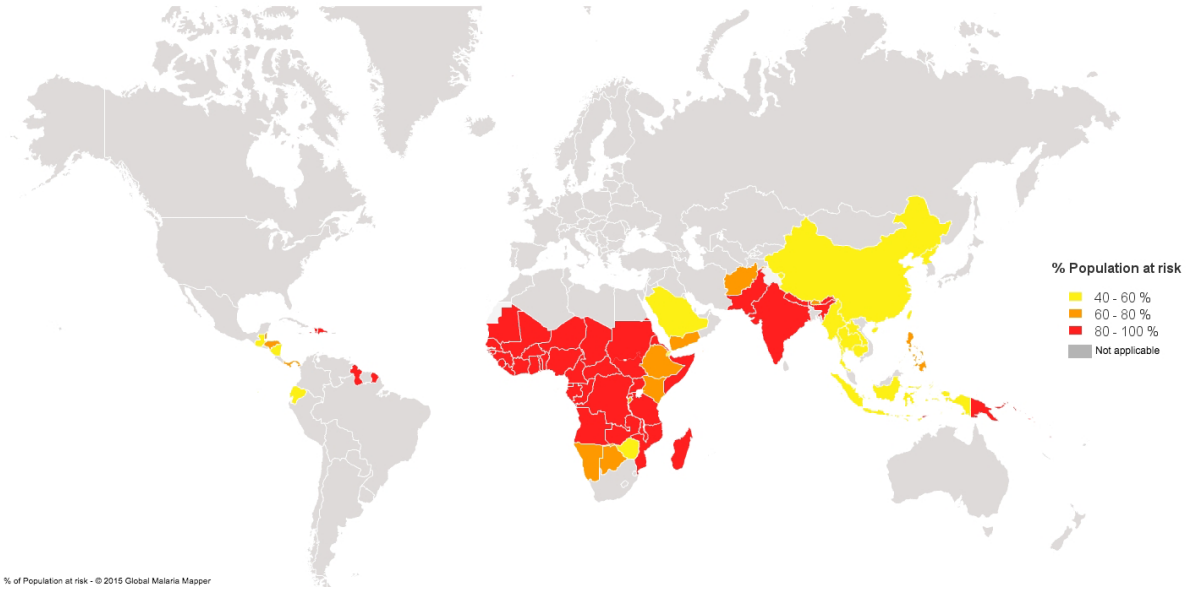

Figure 1. Global distribution of malaria in terms of the populations at risk (WHO, 2015). The regions affected by malaria are coloured based on the percentage of total population at risk.

1.2 Therapies and preventative measures against malaria

1.2.1 Drug therapy

There are currently three different classes of antimalarials mainly used in for drug therapy: quinolines, antifolates, and artemisinin derivatives (Petersen et al., 2011).

Quinine was first isolated in 1820 from the bark of the cinchona tree for treatment of chills and fevers (Butler et al., 2010). The compound was eventually synthesized and derivatives, such as chloroquine and mefloquine, and atovaquone were developed. Chloroquine accumulates in the digestive vacuole or food vacuole of the parasite during the intraerythrocytic stages (Sullivan et al., 1996). Within the digestive vacuole, the parasite digests hemoglobin, releasing hematin, which is the dimer of heme (Fitch et al., 2004). Unless the hematin is detoxified and converted into hemozoin crystals, hematin accumulation is lethal towards the parasite. Chloroquine targets this pathway, where it binds to hematin within the food vacuole. This inhibits the conversion of hematin into hemozoin crystals, leading to accumulation of hematin and thus parasite death (Egan et al., 2008). However, chloroquine resistant *P. falciparum* strains were first observed in the 1950s, and are currently present in almost all endemic areas (Petersen et al., 2011). This resistance is rendered by a polymorphism in the chloroquine resistance transporter (*Pf*CRT) (Sidhu et al., 2002) as well as increased expression of P-glycoprotein homologue 1, which is associated with multidrug resistance (*Pf*MDR1) (Barnes et al., 1992).

Another class of antimalarial drug are antifolates, including sulfadoxine, dapsone, pyrimethamine, and proguanil. After chloroquine resistance parasite strains emerged, a synergistic combination of sulfadoxine-pyrimethamine was used as the front-line drug treatment (Chulay et al., 1984). These two drugs target two different pathways. Sulfadoxine inhibits dihydropteroate synthetase enzyme (*Pf*DHPS), which is part of the biosynthesis pathway of folate (Triglia & Cowman, 1994); pyrimethamine targets dihydrofolate reductase (*Pf*DHFR), a component of the dTMP synthesis pathway required for DNA synthesis as well as maintaining intracellular tetrahydrofolate levels (Bzik et al., 1987). Unfortunately, sulfadoxine-pyrimethamine resistance in *P. falciparum* parasites also emerged shortly after introduction of these new compounds, (Plowe et al., 1998), leaving artemisinin based therapy to be the front-line choice of medication against falciparum malaria (Petersen et al., 2011).

Some artemisinin derivatives that are currently clinically used are dihydroartemisinin, artemether, and artesunate (Petersen et al, 2011). Artemisinin combination therapy (ACT) is currently used as the first choice of drug therapy and prophylaxis, where artemisinin derivatives are administered in combination with other drugs such as quinolines (Hasugian et al., 2007). Two types of ACTs used are dihydroartemisinin-piperaquine and artesunate-amodiaquine (Hasugian et al., 2007). These treatments are able to quickly decrease an individual's parasitemia, where artemisinin derivatives are bioactivated and release free radicals which interfere with the parasites' biological processes (Meshnick, 2002). This involves damaging alkylation processes and hindering the conversion of heme into hemozoin crystals (Kannan et al., 2002). However, *P. falciparum* resistance against artemisinin has already been observed in southeast Asia (Tun et al., 2015), a reminder that it is of high priority to discover new drugs and drug candidates.

1.2.2 Vector control

P. falciparum is transmitted by female *Anopheles* mosquitoes, which are widely distributed in African, middle East Asian, South Asian, Southeast Asian, and South American regions (Kiszewski et al., 2004). Drastic reduction and eradication of malaria is possible by preventing transmission of the malaria parasite from the mosquito to humans. Insecticides of biological, natural and chemical origin, as well as destruction, controlling and monitoring the breeding ground of the mosquitoes play a pivotal role in this counter measurement (Raghavendra et al., 2011).

The most prominent insecticide is dichlorodiphenyltrichloroethane (DDT). DDT was used in aerial spraying campains until the 1970's, and is now only used in indoor residual spraying (IRS), where the chemical can kill the mosquito as well as acting as a repellent (Bouwman et al., 2011). Although it has been estimated to prevent millions of malaria cases (Mabaso et al., 2004), due to its toxicity towards humans and its categorization as one of the persistent organic pollutants (POPs), DDT use is still controversial (Raghavendra et al., 2011).

Mosquito bite prevention is another highly efficient additional counter measurement. The use of insecticide-treated nets (ITNs) has shown a 35% decrease in child mortality after implementation in Tanzania within a four year period (Masanja et al., 2008).

1.3 Biology of *Plasmodium falciparum*

1.3.1 Life cycle of *P. falciparum*

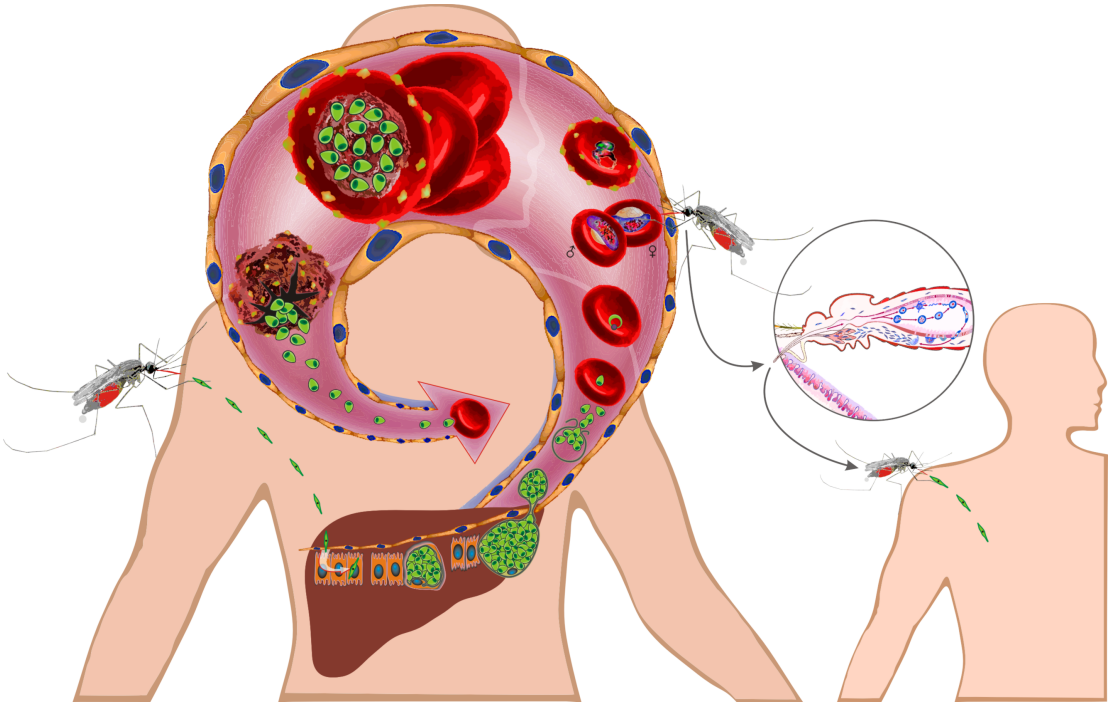

Figure 2. Asexual and sexual life cycle of the *P. falciparum* parasite. Once the sporozoites enter the human host, the parasite undergoes two rounds of asexual replication: i) in the hepatocyte and ii) in the erythrocyte. When the infected individual is bitten by a female *Anopheles* mosquito, the female and male gametes fused within the midgut of the mosquito, beginning sexual proliferation within the mosquito host.

The apicomplexan parasite has a two phases to its life cycle- the sexual and asexual phases (Figure 2). The sexual phase occurs within the mosquito host, where the parasite develops into a sporozoite, which resides in the salivary gland of a female *Anopheles* mosquito. During a blood meal, sporozoites are transmitted into the human blood stream via the mosquito's saliva, where they then travel to the liver, sequentially invading a hepatic cell.

The liver cell is the first site of asexual mass proliferation, where one sporozoite can develop into an exo-erythrocytic schizont, eventually producing more than ten thousand daughter merozoites (Farrow et al., 2011). Once matured, the hepatic cell ruptures, releasing daughter merozoites in merosomes- vesicles which bud off the hepatic cell. The merosome offers protection for the parasite against the host immune system, allowing safe entrance of the merozoites into the blood circulation (Sturm et al., 2006). Once in the blood stream, the merosome ruptures, freeing merozoites that can then invade red blood cells (RBCs).

From this point, the parasite can either enter the asexual intraerythrocytic stages or gametocytogenesis. The decision is dependent on the environment of the human host and the resources available for parasite growth. For example, a high parasitemia will lead to a stressful environment due to the lack of healthy red blood cells, and merozoites will favor gametocytogenesis over asexual proliferation in the blood stages (Sutherland et al., 2009). The production of gametocytes is extremely important, as they are the pre-sexual forms for sexual proliferation after uptake into the mosquito host via a blood meal. In the mosquito host, gametocytes can differentiate into approximately eight male microgametes or one female macrogamete, a process termed as gametogenesis (Bousema & Drakeley, 2011). Fertilization of the macrogamete by a microgamete occurs within the midgut of the mosquito, forming a zygote. The zygote then matures into an ookinete, which buds off from the midgut wall as an oocyst (Bousema & Drakeley 2011). One *P. falciparum* oocyst can produce and release approximately 3000 sporozoites, which travel to the mosquito salivary gland (Rosenberg & Rungsiwongse, 1991).

Instead of progressing through gametocytogenesis, the parasite can decide to proceed through the intraerythrocytic cycle, which spans a time period of approximately 48 hours in the case of *P. falciparum*. The intraerythrocytic cycle is significant to the overall disease as it is responsible for all the clinical symptoms of malaria. Once the parasite has invaded the red blood cell, parasitic proteins are exported into the infected red blood cell (iRBC), such as the knob-associated His-rich protein (KAHRP) (Maier et al., 2009). The export of this protein helps to alters the iRBC surface morphology, resulting "knobs" on the erythrocyte surface (Leech et al., 1984). Part of these knob structures is the

erythrocyte membrane protein 1 (*Pf*EMP1), which is coded by the *var* multigene family that contributes to virulence variation of the parasite (Gardner et al., 2002). *Pf*EMP1 is able to bind with its extracellular domain to various endothelial receptors such as the intercellular adhesion molecule 1 (ICAM-1) and CD36 (Baruch et al., 1996). These surface exposed parasite proteins lead to cytoadherence, preventing blood circulation in critical organs such as the brain and kidney, leading to coma and organ failure (Waller et al., 1995).

During this asexual multiplication, the parasite takes different forms. At 0-12 hours post invasion (hpi), the parasite is in a form of a ring, which then matures into a trophozoite at 24 hpi, and finally in into a schizont at approximately 36 hpi (Maier et al., 2009). Schizonts are defined as multi-nuclear cells, and are the point of the intraerythrocytic cycle when the formation of daughter merozoites occur. One schizont can produce up to 32 merozoites, which burst out of the iRBC once matured, where the free merozoites enter the blood stream once again to invade healthy erythrocytes.

1.3.2 Invasion of merozoites into erythrocytes

The invasion process was visualized in detail by Aikawa and colleagues in 1978 using electron microscopy (EM) revealing four distinct steps: attachment to the erythrocyte membrane, reorientation so the apical end is facing towards the erythrocyte, tight junction formation, and ingress into the host cell (Aikawa et al., 1978). This was supported by more recent work using video microscopy, showing that the entire invasion process takes approximately 40 seconds (Yahata et al., 2012).

One protein involved in the initial attachment is the merozoite sfiurface protein 1 (MSP1). MSP1 is expressed on the merozoite surface (Holder et al., 1992; Perkins & Rocco, 1988; Herrera et al., 1993). Secure attachment of the merozoite to the erythrocyte is mediated by parasitic reticulocyte homology (RH) and Duffy binding-like ligands (DBL) interacting with erythrocyte surface receptors (Srinivasan et al., 2011). This irreversible attachment is initiated by the secretion of RH, DBL, and other proteins from the apical secretory organelles such as the dense granules, micronemes and rhoptries (Figure 3). For example, the rhoptry neck proteins (RON) including RON2 are released from the rhoptries, inserted into the erythrocyte membrane and interacts with type I transmembrane proteins that are translocated to the plasma membrane of the parasite, such as apical membrane antigen 1 (AMA1) (Cao et al., 2009).

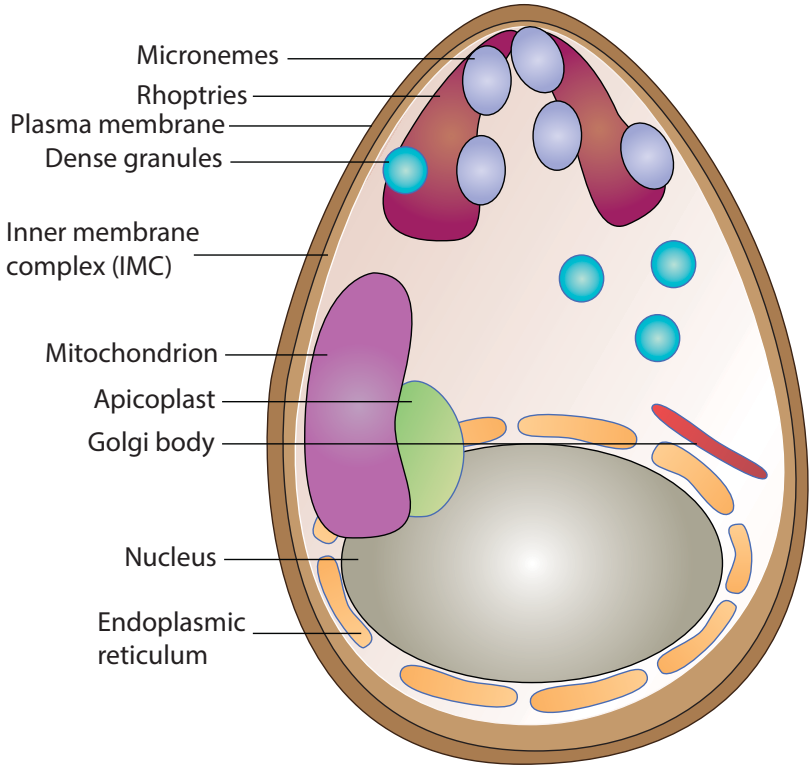

Figure 3. Structure of a *P. falciparum* merozoite. As a eukaryotic cell, a merozoite contains the main organelles such as the nucleus, endoplasmic reticulum, and the mitochondria. The parasite also contains a set of secretory organelles located at the apical end, namely the micronemes, rhoptries, and dense granules. The merozoite also possesses a unique organelle to the superphylum of Alveolates, called the inner membrane complex (IMC), a double membrane system (not shown in schematic) directly underlying the plasma membrane.

It is not entirely clear how these ligand-receptor protein complexes are linked to the actin-myosin motor of the malaria parasite, but it is evident that the actin-myosin motor of the parasite generates the driving force (Farrow et al., 2011).

1.3.3 The genome and invadome of the *P. falciparum*

The entire *Plasmodium falciparum* genome is composed of 23 mega-base pairs packed into 14 chromosomes. *P. falciparum* has the most AT-rich genome known to date, and codes for 5,268 proteins (Gardner et al., 2002). Transcriptional regulation is meticulous in the parasite, where proteins are expressed during specific stages depending on its function (Florens et al., 2002). 3.9% of the genome is dedicated in host cell immune invasion, while at least 1.3% of the genome is responsible for the invasion process and host-cell interactions (Gardner et al., 2002). With bioinformatics, a network of 418 proteins was predicted to contribute to the invasion process of *P. falciparum* into erythrocytes, where seven of these proteins localize to the IMC (Hu et al., 2010).

1.3.4 The inner membrane complex (IMC) and the glideosome

The actin myosin motor is anchored to the inner membrane complex (IMC), a feature unique to the phylogenetic group of unicellular organisms called the alveolata which includes the phyla Ciliophora, Dinoflagellata, and Apicomplexa (Cavalier-Smith, 1993). This endomembrane system consists of a double phospholipid layer underlying underlying the plasma membrane. The intermembrane space between the plasma membrane and the IMC is thought to be approximately 20-25nm as predicted in *Toxoplasma gondii*, another apicomplexan parasite (Frenal et al., 2010). The entire IMC is structurally supported by cytoskeletal microtubules on the inner face of the double membrane layer (Figure 5; Morrissette & Sibley, 2002).

The biogenesis of the IMC is Golgi derived and starts during the late stage of schizogony, approximately seven hours prior to the rupture of the iRBC (Kono et al., 2012). During this process, three morphological distinct forms can be visualized by microscopy (Kono et al., 2012; Ridzuan et al., 2012). As presented in Figure 4, during the first stage (T1), the IMC appears at the apical end of the nascent merozoites in the form of cramps. In the subsequent maturation step (T2), each cramp closes into rings. This ring then extends in a lateral fashion that might be connected to the invagination of the plasma membrane (Gilberger laboratory, unpublished), resulting in a peripheral double membrane layer underneath the plasma membrane (T3) of each individual daughter merozoite within the schizont (Kono et al., 2012).

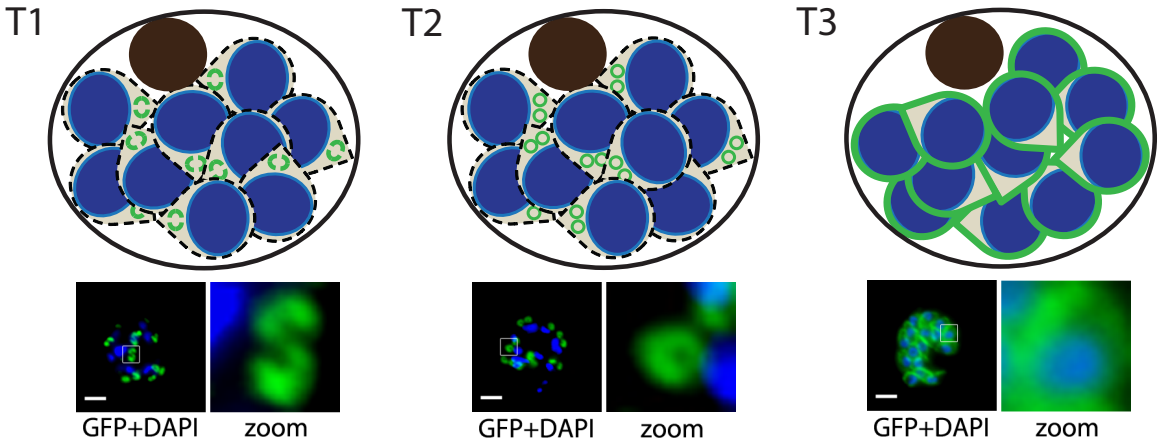

Figure 4. Biogenesis of the IMC within a merozoite. Development of the IMC occurs during the late intraerythrocytic cycle in three stages: T1, T2, and T3. In the T1 stage, the IMC takes form of cramp, which then develop into doughnut-like shapes (T2). At the T3 stage, the IMC directly underlies the plasma membrane, indistinguishable from a plasma membrane phenotype under 100x magnification. In the simplified schematics, the parasite food vacuole is in brown, DAPI-stained nuclei is in blue, black dotted lines represent an unformed nascent merozoite plasma membrane, and the black solid lines represent the erythrocyte membrane. In the live microscopy images, blue represents the DAPI-stained nuclei; scale bar, 2 μm.

There are more than 30 IMC proteins identified to date, reflecting the multiple function of the IMC such providing a scaffold for daughter cell formation, maintaining cell morphology, and cell motility (Kono et al., 2012). The IMC functions as a physical

anchor for the actin-myosin motor, termed “glideosome”, allowing the merozoite to invade red bloods cells (Opitz & Soldati, 2002).

Well-characterized components of the glideosome include Myosin A (MyoA), myosin A tail interacting protein (MTIP), and the glideosome associated proteins (GAPs) GAP45 GAP50 (Gaskin et al., 2004). GAP45, MTIP, and MyoA are assembled in the cytosol as a “proto-glideosome” (Gaskin et al., 2004), while GAP50 is embedded into the IMC membrane (Bosch et al., 2012). The C-terminal tail of GAP50 is required to anchor the proto-glideosome to the IMC, possibly via the interaction between GAP50 and GAP45. (Gaskin et al., 2004) (Figure 5). GAP45 encodes N- and C-terminal lipidation motifs that are implicated with IMC membrane association. One model for the topology of GAP45 portrays GAP45 to be spanning the intermembrane space between the outer membrane of the IMC and the plasma membrane (Frenal et al., 2010).

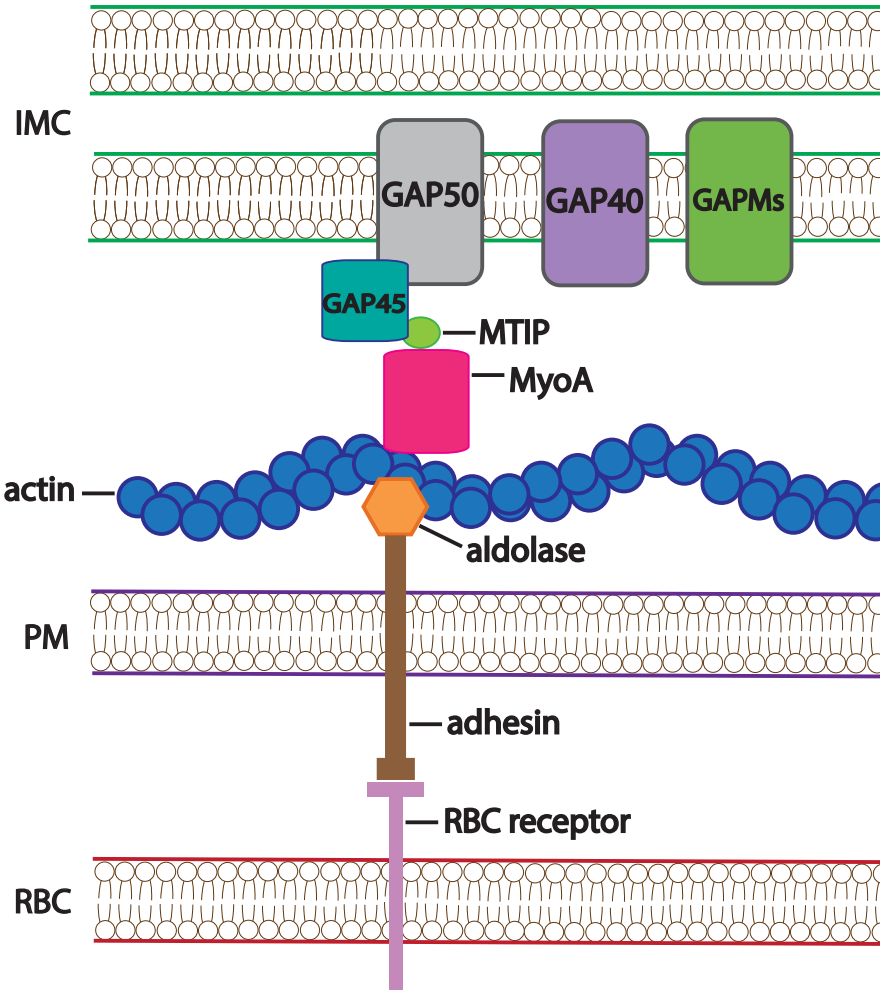

Figure 5. Model of the invasion machinery in *P. falciparum*. The parasite attaches to the red blood cell (RBC) receptors through adhesion proteins, which are connected to the invasion machinery via aldolase. The glideosome functions based on an actin-myosin motor, and the main known components of the glideosome are Myosin A (MyoA), Myosin A tail interacting protein (MTIP), and the glideosome associated proteins (GAP45 and GAP50). Other glideosome associated proteins such as GAP40 and the glideosome associated proteins with multiply membrane spans (GAPMs) (Bullen et al., 2009) are also localized to the IMC, but how they are assembled with the rest of the glideosome components are unknown.

1.3.5 Role of lipid modification and phosphorylation for membrane recruitment in *P. falciparum*

1.3.5.1 Myristoylation and palmitoyaltion

The mode of membrane targeting in *P. falciparum* seems to vary depending on the target organelle, but generally targeting to a membrane is dependent on the N-terminal dual acylation motif, consisting of myristoylation and palmitoylation modifications. For example, the Armadillo Repeats-Only protein (ARO), a rhoptry protein, and the IMC sub-compartment proteins (ISPs), *Pf*ISP1 and *Pf*ISP3, require both N-terminal myristoylation and palmitoylation for general membrane association (Cabrera et al., 2012; Wetzel et al., 2015).

N-Myristoylation is a co-translational and irreversible modification, where a myristate, a 14-carbon fatty acid, is transferred from myristoyl coenzyme A to the target protein via an amide bond (Cabrera et al., 2012). This reaction is catalyzed by N-Myristoyltransferase (NMT), where the N-terminal glycine positioned second to the initial methionine is targeted. In *P. falciparum*, 2% of the proteome is predicted to be myristoylated (Wright et al., 2014). N-myristoylation is key to protein localization through membrane association, and it is found that inhibition of NMT activity leads to disrupted assembly of the IMC, resulting in parasite death (Wright et al., 2014).

After the protein has docked to a membrane via myristoylation, the interaction is further stabilized via palmitoylation. Palmitoylation is a reversible post-translational modification, where a 16-carbon palmitate, is added to cysteine residues through thioester bonds (Jones et al., 2012a). Using metabolic labeling/click chemistry (MLCC) and Acyl-Biotin Exchange (ABE) methods, palmitoylated proteins were enriched and identified using mass spectrometry in *P. falciparum.* 33% of all parasite proteins (1,752 proteins out of 5,268 proteins) are palmitoylated in the late intraerythryocytic stages (Jones et al., 2012a). Palmitoylation plays a role in protein stability, protein-protein interaction, as well as membrane association.

This reaction is catalyzed by palmitoyl-acyl transferases (PATs), where one family of PATs is the DHHC family (Jones et al., 2012b). DHHC PATs have a conserved Asp-His-His-Cys domain, where 12 are expressed in *P. falciparum* (Jones et al., 2012b). However, how the specificity of the protein substrate is determined is still unknown (Jones et al., 2012a). One possibility is the membrane specificity of PATs. DHHC PATs are integral

membrane proteins, containing four to six transmembrane domains. Recently, an IMC PAT, *Pf*DHHC1, has been described (Wetzel et al., 2015), which could possibly be responsible for the palmitoylation of IMC proteins or proteins of close proximity.

1.3.5.2 Phosphorylation

Finally, the last type of protein modification that plays a role in this thesis is phosphorylation. Protein phosphorylation is a well-established regulator in biological processes, which is also true in many regulatory events in *P. falciparum* including the invasion process. This is apparent as the inhibition of serine/threonine kinases results in decreased merozoite invasion into erythrocytes (Jones et al., 2009). In late intraerythrocytic stages, 919 phosphorylated proteins were identified, including the glideosome components myosin A and GAP45 (Lasonder et al, 2012).

Phosphorylation is catalyzed by kinases, and the *P. falciparum* encodes for 99 protein kinases (Anamika et al., 2005). *P. falciparum* lacks tyrosine specific kinases, but has 65 kinases which can be classified as part of the eukaryotic protein kinase family, such as casein kinase 1 (CK1) and calcium/calmodulin-dependent protein kinase (CaMK) groups (Solyakov et al., 2011). Among the 65 kinases, 36 kinases expressed during schizogony are essential for parasite survival (Solyakov et al., 2011). GAP45 was shown to be phosphorylated *in vivo* at the residues S89, S103, S107, S142, S149, 156, T158, and S198 (Treeck et al., 2011), and is a substrate of protein kinase A (*Pf*PKA) (Lasonder et al., 2012), protein kinase B (*Pf*PKB) (Thomas et al., 2012), and calcium-dependent protein kinase 1 (CDPK1) (Green et al., 2008; Thomas et al., 2012).

1.3.6 Current crystal structures of the glideosome

One way to further understand the assembly of the glideosome would be to gain structural insight. Currently, there are over 75 apicomplexan protein structures available, where approximately 30 crystal structures are of components of the glideosome (Boucher & Bosch, 2015) such as aldolase (Kim et al., 1998), actin (Vahokoski et al., 2014), the MyoA peptide with MTIP (Bosch et al., 2007; Douse et al, 2012; Douse et al., 2013), and GAP50 (Bosch et al., 2012). However, it is notable that the GAP45 structure is missing, which would help to understand the probable interaction with GAP50.

1.4 Objectives

GAP45 is an essential member of the glideosome (Frenal et al., 2010). To elucidate its role in the glideosome, the protein was dissected in terms of its modifications: the N-terminal dual-acyl lipidation motifs, the C-terminal cysteine residues which may participate in palmitoylation, and phosophorylation. Additionally, structural insight will be initiated by production and purification of recombinant GAP45 for crystallization studies.

2. Materials

2.1 Chemicals

Acetic acid	Roth, Karlsruhe
Acetone	Merck, Darmstadt
Acrylamide/Bisacrylamide solution (40%)	Roth, Karlsruhe
Agar-Agar	Becton Dickinson, Heidelberg
Agarose	Eurogentec, Seraign, Belgium
AlbumaxII	Invitrogen, Karlsruhe
Albumin bovine Fraction V (BSA)	Biomol, Hamburg
Ampicillin	Roche, Mannheim
Bacto™ yeast extract	Becton Dickinson, Heidelberg
Bacto™ Pepton	Becton Dickinson, Heidelberg
Blasticidin S	Invitrogen, Karlsruhe
Bromphenol blue	Merck, Darmstadt
Deoxynucleotides (dNTPs)	Fermentas, St. Leon-Rot
4',6-diamidino-2-phenylindole (DAPI)	Roche, Mannheim
Digitonin	Sigma-Aldrich, Steinheim
Dimethyl sulfoxide (DMSO)	Sigma-Aldrich, Steinheim
Dipotassium phosphate	Roth, Karlsruhe
Disodium phosphate	Roth, Karlsruhe
1,4,-dithiothreitol (DTT)	Roche, Mannheim
Ethanol	Merck, Darmstadt
Ethidium bromide	Sigma-Aldrich, Steinheim
Ethylenediamine tetraacetic acid	Biomol, Hamburg
Ethyleneglylcol tetraacetic acid	Merck, Darmstadt

Gentamycin	Ratiopharm, Ulm
Giemsas azur eosin methylene blue solution	Merck, Darmstadt
D-Glucose	Merck, Darmstadt
Glutaraldehyde (25%)	Roth, Karlsruhe
Glycerol	Merck, Darmstadt
Glycine	Biomol, Hamburg
HEPES	Roche, Mannheim
Hyoxanthin	Merck, Darmstadt
Imidazole	Roth, Karlsruhe
Isopropyl-beta-D-thiogalactopyranoside (IPTG)	Roth, Karlsruhe
Isopropanol	Merck, Darmstadt
Kanamycin sulfate	Sigma-Aldrich, Steinheim
Magnesium chloride	Merck, Darmstadt
Methanol	Merck, Darmstadt
Milk powder	Roth, Karlsruhe
3-(N-morpholino)-Propansulfonic acid (MOPS)	Merck, Darmstadt
N, N, N', N'-Tetramethylethylenediamine (TEMED)	Merck, Darmstadt
Nonidet P-40	Sigma-Aldrich, Steinheim
Potassium chloride	Merck, Darmstadt
Protease inhibitor cocktail tablets	Roche, Mannheim
RPMI (Roswell Park Memorial Institute)- Medium	Invitrogen, Karlsruhe
Saponin, from quillaja bark	Serva, Heidelberg
Sodium acetate	Merck, Darmstadt
Sodium bicarbonate	Sigma-Aldrich, Steinheim

Sodium chloride	Gerbu, Gaiberg
Sodium dodecyl sulfate (SDS)	Serva, Heidelberg
Sodium dihydrogen phosphate	Roth, Karlsruhe
Sodium hydroxide	Merck, Darmstadt
D-Sorbitol	Sigma-Aldrich, Steinheim
Trichloroacetic acid (TCA)	Merck, Darmstadt
Tris(2-carboxyethyl)phosphine hydrochloride (TCEP)	Thermo Scientific Pierce, Rockford
Tris base	Roth, Karlsruhe
Tris-HCL	Promega, Madison
Triton-X-100	Biomol, Hamburg
Tween® 20 detergent	Merck, Darmstadt
WR99210	Jacobus Pharmaceuticals, Maryland, USA
Xylene cyanol	Sigma-Aldrich, Steinheim

2.2 Kits

NucleoSpin®Plasmid	Macherey-Nagel, Düren
NucleoSpin®Extract II	Macherey-Nagel, Düren
Plasmid Midi Kit	Qiagen, Hilden
QIAamp® DNA Mini Kit	Qiagen, Hilden
Western Blot ECL-Detection Kit	Thermo Fisher Scientific, Schwerte

2.3 DNA and protein ladders

GeneRuler^{TM}1000bp ladder	Fermentas, St. Leon
PageRuler^{TM}Prestained protein ladder	Fermentas, St. Leon

PageRuler^{TM}Prestained protein ladder	Fermentas, St. Leon
Roti®-Mark Prestained protein ladder	Roth, Karlsruhe

2.4 Stock solutions, buffers, and media

2.4.1 Media and buffers for microbiological experiments

Ampicillin stock	100 mg/ml in 70% ethanol
Glycerol stabilate (freezing)	50 % (v/v) glycerol in dH_2O
IPTG stock	1M IPTG in dH_2O
Kanamycin stock	50 mg/ml in dH_2O
LB-medium	1 % (w/v) NaCl, 0.5 % (w/v) peptone 1 % (w/v)Yeast extract in dH_2O
LB-agar plates	1.5 % (w/v) agar-agar in LB medium
LB-Ampicillin selection media	Autoclaved LB-medium or LB-agar 100 μg/ml of ampicillin
LB-Kanamycin selection media	Autoclaved LB-medium or LB-agar 50 μg/ml of kanamycin
TFBI buffer	30 mM acetic acid

	50 nM $MnCl_2$ 100 mM RbCl 10 mM $CaCl_2$ 15 % (v/v) Glycerin pH 5.8 (with acetic acid)
TFBII buffer	10 mM MOPS 75 mM $CaCl_2$ 10mM RbCl 15 % (v/v) Glycerin pH 7.0

2.4.2 Buffers and solutions for molecular biological experiments

6 X DNA loading dye	40 % (v/v) glycerol 2.5 % (w/v) xylene cyanol 2.5 % (w/v) bromphenol blue in dH_2O
CutSmart® Buffer	NEB, Ipswich, USA
20 mM dNTP	Solis Biodyne, Tartu, Estonia
25 mM $MgCl_2$	Solis Biodyne, Tartu, Estonia
Phusion® HF Buffer	NEB, Ipswich, USA

Reaction Buffer BD	Solis Biodyne, Tartu, Estonia
Sodium acetate	3 M NaAc, pH 5.2
T4 DNA Ligase Reaction Buffer	NEB, Ipswich, USA
50 X TAE	2 M Tris-Base 1 M glacial acetic acid 0.05 M EDTA pH 8.5
Tris EDTA (TE) buffer	10 mM Tris-HCl pH 8.0 1 mM EDTA pH 8.0

2.4.3 Media, buffers and solutions for cell biological experiments

Blasticidin S (BSD) solution	5 mg/ml BSD in RPMI complete medium sterile filtration
Formaldehyde/glutaraldehyde fixation solution	40 % (v/v) 10 % formaldehyde 0.03 % (v/v) 25 % glutaraldehyde 10 % (v/v) 10 X PBS in dH_2O
10 % Giemsa stain	10 % (v/v) Giemsas Azur-Eosin-Methylenblue-solution

	in dH_2O
Human red blood cells	Sterile human erythrocyte concentrate; blood group O+ (blood bank Universitätsklinikum Eppendorf (UKE), Hamburg)
Malaria freezing solution (MFS)	4.2 % (w/v) D-Sorbitol 0.9 % (w/v) NaCl 28 % (v/v) Glycerol sterile filtration
Malaria thawing solution (MTS)	3.5 % (w/v) NaCl in dH_2O sterile filtration
10 X PBS	200 mM $Na_2HPO_4 \bullet 2H_2O$ 52 mM $NaH_2PO_4 \bullet 2H_2O$ 1.3M NaCl pH 7.4 autoclave
1 X PBS	1:10 dilution of 10 X PBS in dH_2O
RPMI- complete medium	1.587 % (w/v) RPMI 1640 12 mM $NaHCO_3$ 6 mM D-Glucose

	0.5 % (v/v) Albumax II 0.2 mM Hypoxanthine 0.4 mM Gentamycin pH 7.2 sterile filtration
Saponin lysis buffer	0.03 % (w/v) Saponin in 1 X PBS
Synchronization solution	5 % (w/v) D-Sorbitol in dH_2O sterile filtration
WR99210 stock solution	20 mM in 1 mL DMSO sterile filtration

2.4.4 Stock solutions, buffers for biochemical experiments

2.4.4.1 Protein separation using SDS-PAGE

Ammoniumpersulfate (APS)	10 % APS (w/v) in dH_2O
1 X Running buffer	1:10 dilution of 10X running buffer in dH_2O
5 X SDS sample buffer	375 mM Tris-HCl, pH 6.8 12 % (w/v) SDS 60 % (v/v) Glycerol 0.6 M DTT 0.06 % (w/v) Bromphenol blue

Separating gel buffer	1.5 M Tris-HCl, pH 8.8
Separating gel (10 %)	1.5 ml separating gel buffer 2.5 ml dH_2O 2 ml Acrylamide (40%) 60 µl (w/v) SDS (10%) in dH_2O 25 µl (w/v) APS (10%) in dH_2O 5 µl TEMED
Stacking gel buffer	1 M Tris-HCl, pH 6.8
Stacking gel (4 %)	1 ml stacking gel buffer 2.5 ml dH_2O 0.5 ml Acrylamide (40%) 40 µl (w/v) SDS (10%) in dH_2O 20 µl (w/v) APS (10%) in dH_2O 5 µl TEMED

2.4.4.2 Buffers for protein transfer (Western blot)

Blocking solution	5 % (w/v) milk powder in 1 X PBS
Coomassie solution	0.025 % (w/v) Coomassie Brilliant Blue R-250 10 % (v/v) acetic acid

	45 % methanol
	in dH_2O
Wash Buffer	1 X PBS
	0.05% Tween 20
10 X Wet transfer buffer	250 mM Tris base
	1.92 M Glycine
	0.037 % (w/v) SDS
	in dH_2O
1 X Wet transfer buffer	100 ml 10 X wet transfer buffer
	200 ml Methanol
	700 ml dH_2O

2.4.4.3 Buffers and solutions for protein purification (FPLC)

Buffer A	20 mM Tris, pH 7.5
	20 mM imidazole
	150 mM NaCl
	5 % Glycerol
	0.5 mM TCEP
Buffer B	20 mM Tris, pH 7.5
	500 mM imidazole
	150 mM NaCl
	5 % Glycerol

	0.5 mM TCEP
Dialysis buffer	20 mM Tris, pH 7.5
	150 mM NaCl
	5 % Glycerol
Gel filtration buffer	20 mM Tris, pH 7.5
	150 mM NaCl
	5 % Glycerol
	0.5 mM TCEP
Lysis buffer	50 mM Tris, pH 7.5
	20 mM imidazole
	300 mM NaCl
	10 % Glycerol
	5 U/ml DNaseI
	0.5 mM TCEP
	1X protease inhibitor cocktail
Wash buffer	20 mM Tris, pH 7.5
	20 mM imidazole
	1 M NaCl
	5 % Glycerol
	0.5 mM TCEP

25 X Protease inhibitor cocktail	1 protease inhibitor cocktail 400 μL dH_2O

2.4.4.4 Buffers and solutions for solubility assay

Sodium carbonate buffer	0.1 M Na_2CO_3 in dH_2O
Triton-X-100 buffer	1 % Triton-X-100 in 1 X PBS

2.4.4.5 Buffers and solutions for Proteinase K protection assay

SoTE	0.6 M sorbitol 20 mM Tris-HCl, pH 7.5 1 mM EDTA
0.02% Digitonin	0.02% Digitonin in SoTE
Proteinase K	0.1 mg/mL Proteinase K in SoTE

2.5 Bacterial and *Plasmodium* strains

2.5.1 Bacterial strains

Escherichia coli XL10-Gold	Tetr**Δ**(*mcrA*)183**Δ**(*mcrCB-hsdSMRmrr*) 173*endA1 supE44 thi-1 recA1 gyrA96* *relA1 lac* Hte [F'*proAB laclqZ ΔM15 Tn10* (Tetr) Amy Camr]
Escherichia coli BL21(DE3)	*fhuA2 [lon] ompT gal (λ DE3) [dcm]* *ΔhsdS* *λ DE3 = λ sBamHIo ΔEcoRI-B* *int::(lacI::PlacUV5::T7 gene1) i21 Δnin5*

2.5.2 *Plasmodium* strains

Plasmodium falciparum 3D7	MR4, Manasses/ USA, Origin: Africa

2.6 Enzymes

2.6.1 Endonucleases

DNase I [2U/µl]	NEB, Ipswich, USA

2.6.2 Ligases

T4 DNA-Ligase [3U/µl]	NEB, Ipswich, USA

2.6.3 Polymerases

FirePol® DNA Polymerase [5U/µl]	Solis Biodyne, Tartu, Estonia
Phusion® High-Fidelity DNA Polymerase [5U/µl]	NEB, Ipswich, USA

2.6.4 Proteases

Proteinase K [0.8U/µl]	NEB, Ipswich, USA

2.6.5 Restriction enzymes

Fast digest® *BamHI* [20U/µl]	G/GATCC	Fermentas, St. Leon
Fast digest® *NcoI* [20U/µl]	C/CATGG	Fermentas, St. Leon

Fast digest® *NotI* [20U/µl]	GC/GGCCGC	Fermentas, St. Leon
XhoI [20U/µl]	C/TCGAG	NEB, Ipswich, USA

2.7 Antibodies

2.7.1 Primary antibodies

Antigen	Organism	Dilution	Usage	Source
Aldolase	Rabbit	1:2000	Western blot	Bergmann & Spielmann, unpublished
BiP	Rabbit	1:2000	Western blot	Struck et al., 2005
GAPDH	Mouse	1:5000	Western blot	Daubenberger *et al.*, 2000
GAP50	Rabbit	1:500	IFA	Jones et al., 2006
GAPM2	Mouse	1:500	IFA	Kono et al., 2012
GAPM2	Mouse	1:1000	Western blot	Kono et al., 2012
GFP	Mouse	1:1000	Western blot	Roche
RFP [5F8]	Rat	1:1000	Western blot	Chromotek

2.7.2 Secondary antibodies

Antigen	Organism	Dilution	Usage	Source

Mouse	HRP	1:3000	Western blot	Dianova, Hamburg
Rabbit	HRP	1:3000	Western blot	Dianova, Hamburg
Rat	HRP	1:3000	Western blot	Dianova, Hamburg
Mouse	Alexa 488	1:2000	IFA	Molecular Probes, Leiden, Netherlands
Rabbit	Alexa 488	1:2000	IFA	Molecular Probes, Leiden, Netherlands

2.8 Oligonucleotides

All oligonucleotides were synthesized by Sigma-Aldrich, Steinheim. All working primer dilutions were prepared to a final concentration of 10 μM from a 100 μM stock solution, and were stored at -20°C.

2.8.1 Oligonucleotides for cloning

Name	**Sequence**	**Restriction site**
GAP45 wt fw	5'- GCGCGGATCCATGGGAAATA AATGTTCAAG -3'	BamHI
GAP45 wt rv	5'- GATCGCGGCCGCGCTCAATAAAGGTGTATCG -3'	NotI
GAP45 C160A fw	5'- CATCGAGTTTATTCATATCAGCAGGTGTTACAGATCTATAAG -3'	/
GAP45 C160A rv	5'- CTTATAGATCTGTAACACCTGCTGATATGAATAAACTCGATG -3'	/
GAP45 C176AC178A fw	5'- TAAAGTTTTTTCAAGAAGAGCTGGAGCTGATCTTGGTGAACGTCATG -3'	/
GAP45 C176AC178A rv	5'- CATGACGTTCACCAAGATCAGCTCCAGCTCTTCTTGAAAAAACTTTA -3'	/
GAP45 C178A fw	5'- GTTTTTTCAAGAAGATGTGGAGCTGATCTTGGTGAACGTCATG -3'	/
GAP45 C178A rv	5'- CATGACGTTCACCAAGATCAGCTCCACATCTTCTTGAAAAAAC -3'	/

GAP45 C189A rv	5'- GATCGCGGCCGCGCTCAATAAAGGTGTATCG GATAAATCAATTTTTCTACAAATTTTAGCTGCATTTTC -3'	NotI
GAP45 C192A rv	5'- GATCGCGGCCGCGCTCAATAAAGGTGTATCGGATAAATCAATTTTTCTAG CAATTTTACATGC -3'	NotI
del29aaGAP45 fw	5'- GCGCGGATCCATGCAATCTGAAGAAATAATTGAAGAAAAACC -3'	BamHI
GAP50 C HIS fw	5'- CGCGCCATGGCTTCAAGAAGCAAAGTAAAGG -3'	NcoI
GAP50 C HIS rv	5'- CGTGCTCGAGGCTCAATAAAGGTGTATC -3'	XhoI

All underlined sequences indicate the restriction site for the respective restriction enzyme

2.8.2 Oligonucleotides for sequencing

Name	**Sequence**
ama1 fw	5'- CCTAATAATTTATTTGATAATTTTTC -3'
mCherry rv	5'- GCGCATGAACTCCTTGATGATGGC-3'
pET28a fw	5'-GGGAATTGTGAGCGGATAACAATTCC-3'
pET28a rv	5'-GTTTAGAGGCCCCAAGGGGTTATG-3'

2.9 Vectors

2.9.1 pBcamR

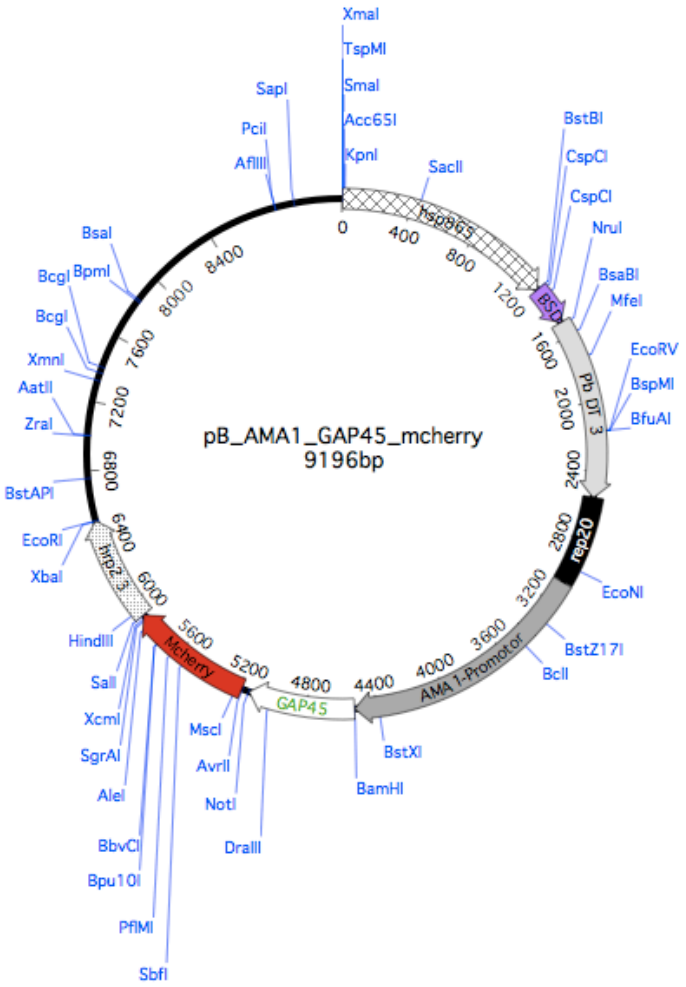

Figure 6. pBama1R vector was used for episomal overexpression of protein in *P. falciparum*.

For this thesis, a derivative of the pBcamR vector (Flueck et al., 2010) was used for the expression of all C-terminally mCherry tagged proteins in the *Plasmodium falciparum* 3D7 cell line. The modifications to the original vector were conducted by Dr. Maya Kono, and include changes in the promoter region and reporter tag. The *cam*-promoter and Rep20 repeat sequence were exchanged for the *ama-1* promoter followed by the Rep20 repeat sequence via the restriction sites PstI and BamHI. This enables the gene of interest to be under late transcriptional control, which is subsequently equivalent to protein expression during schizogony in the intraerythrocytic cycle. The second modification to the vector is the substitution of 3xHA tag with the mCherry reporter protein using the NotI/SalI restriction sites. This derivative of the plasmid can be referred to as pBama1R.

Altogether, cloning the gene of interest utilizing the BamHI and NotI restriction sites allows for a C-terminally tagged mCherry protein expressed during schizogony of the intraerythrocytic cycle. This derivative will be referred to in this thesis as Transgenic parasites were selected using blasticidin, where only parasites possessing the plasmid have the blasticidin S deaminase (BSD) gene, conferring resistance against the drug blasticidin S (Mamoun et al., 1999).

2.9.2 pET28a

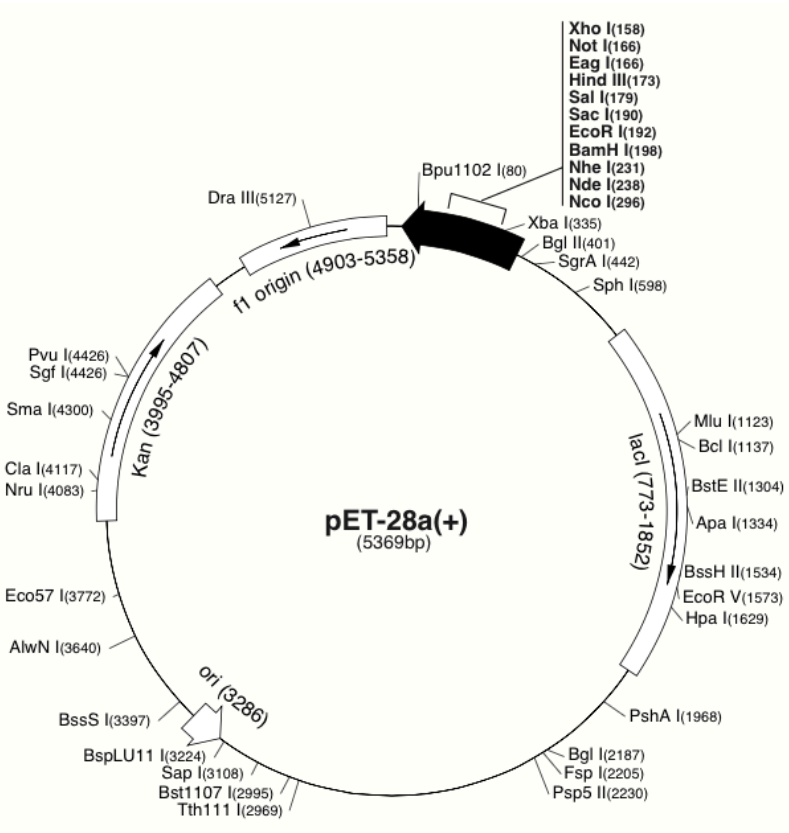

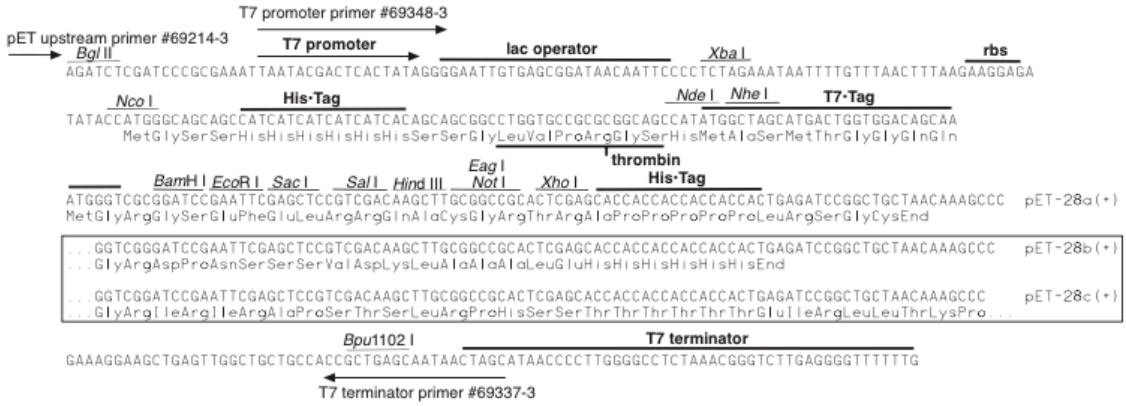

Figure 7. The pET28a vector was used for generating a 6xHIS tagged fusion protein for overexpression in *E. coli*.

The commercially available pET28a vector (Novagen) was used in this thesis for the overexpression of GAP45-HIS, which was then purified for latter crystallization steps. The C-terminally 6xHIS tagged GAP45 construct was produced by cloning GAP45 with the restriction enzymes NcoI and XhoI.

2.10 Sequencing

The sequencing of all GAP45 constructs were completed commercially by MOBIX Lab (McMaster University, Hamilton, Canada), which uses ABI BigDye terminator chemistry.

2.11 Software

Adobe Illustrator CS5	Adobe Systems, San Jose, USA
Adobe Photoshop CS5	Adobe Systems, San Jose, USA
Axio Vision 40 V 4.7.0.0	Zeiss, Jena
ChemiDoc™ XRS+ System with Image Lab™	Bio-Rad, Hercules, USA
CSS-Palm 4.0	Ren et al, 2008
Microsoft Office 2008 for Mac	Microsoft Corporation, Redmond, USA
NMT- The MYR Predictor	Maurer-Stroh et al., 2002
UNICORN™ 6.3	GE Healthcare, Little Chalfont, United Kingdom

3. Methods

3.1 Molecular biological experiments

3.1.1 Polymerase chain reaction (PCR)

PCR amplification of the GAP45 (Gene ID: PFL1090w) gene fragments were conducted using Phusion® High-Fidelity DNA Polymerase (NEB) using the oligonucleotides found in Section 2.8.1. Genomic DNA isolated from *P. falciparum* 3D7 parental cell line was used as the template for all reactions. Reactions were prepared in a final volume of 50 µL containing the reagents in Table 1. The reactions were performed according to the parameters in Table 2.

Table 1: PCR reaction mix for DNA amplification using Phusion polymerase

Reagent	**Volume (µL)**
5X Phusion® HF Buffer	10
dNTP (10 mM)	5
Forward primer (10 µM)	1
Reverse primer (10 µM)	1
Template (1-10ng/µL)	1
Phusion polymerase	0.2
dH_2O	31.8
Final volume	50 µL/reaction

Table 2: PCR parameters for DNA amplification using Phusion polymerase

PCR Step	**Temperature**	**Duration**	**Cycles**
Initialization	98°C	1 min	
Denaturation	98°C	30 sec	35X
Annealing	42°C	40 sec	
Elongation	62°C	1min/1kbp	
Final elongation	62°C	1 min	

Final hold	4°C	forever

3.1.2 Purification of DNA products

3.1.2.1 Purification of PCR products and enzymatic reactions

PCR products were purified from enzymes, primers, nucleotides and salts using the NucleoSpin®Extract II kit (Macherey-Nagel) before and after enzymatic digestion following the manufacturer's protocol. The final PCR product was eluted in 30 μL of dH_2O before the restriction enzyme digest reaction, and eluted in 20 μL of dH_2O after the digest. The final purified product was used for later ligation steps (Section 3.2.4), or was stored at -20°C.

3.1.2.2 Purification of plasmid DNA from agarose gel

The derivative of pBcamR (Flueck et al., 2010), pBama1R, was digested and purified through gel extraction procedures using the NucleoSpin®Extract II kit (Macherey-Nagel). The product was eluted in a final volume of 20 μL, and was either used for later ligation steps (Section 3.2.4), or was stored at -20°C.

3.1.3 Restriction digest of PCR products and plasmids

The PCR products and pBama1R plasmid backbone were digested with 4 U of each BamHI and NotI restriction enzymes in a final volume of 50 μL according to the following recipes (Table 3, Table 4). The BamHI and NotI restriction sites yields in a fusion protein with a mCherry tag at the C-terminus. For validating correct insert size, test digests of plasmid DNA were conducted in a final volume of 20 μL using the same enzymes. All restriction digests were incubated for 1 hour at 37°C.

Table 3: Restriction digest reaction for PCR products

Reagent	**Volume (μL)**
PCR product	25
10X CutSmart® Buffer	5
BamHI	0.2
NotI	0.2
dH_2O	19.6
Final volume	50 μL/reaction

Table 4: Restriction digest reaction for plasmid DNA

Reagent	Volume (μL)
Plasmid DNA (100-200ng/μL)	5
10X CutSmart® Buffer	5
BamHI	0.2
NotI	0.2
dH_2O	39.6
Final volume	50 μL/reaction

3.1.4 Ligation

The final purified pBama1R and PCR product was ligated in a final volume of 10 μL according to Table 5. The concentration ratio of pBama1R and PCR product used was 1:7. The reaction was then incubated at room temperature for 20 min before proceeding to the transformation step (Section 3.2.3).

Table 5: Ligation reaction

Reagent	Volume (μL)
T4 DNA Ligase	1
T4 DNA Ligase Reaction Buffer	1
vector	1
insert	7
Final volume	10 μL/reaction

3.1.5 Screening of bacterial colonies

After the transformation of the plasmid DNA, bacterial colonies with the plasmid containing the correct inserted gene of interest was selected using PCR screening. Colonies on the LB plate with the correct selection drug were numbered, and added into the PCR reaction using a pipette tip. The primers used to screen for the gene of interest inserted into the pBama1R plasmid were ama1 fw and mCherry rv (refer to Section 2.8.2). To screen the gene of interest inserted into the pET28a vector, the primers pET28a

fw and pET28a rv were used (refer to Section 2.8.2). The master mix was prepared for individual 10 μL reactions according to Table 6 and performed as in Table 7.

Table 6: PCR reaction mix bacterial colony screening using FirePol® DNA polymerase

Reagent	Volume (μL)
5X Reaction Buffer BD	2
$MgCl_2$ (25 mM)	2
dNTP (10 mM)	2
Forward primer (10 μM)	1
Reverse primer (10 μM)	1
FirePol® DNA polymerase	0.2
dH_2O	1.8
Final volume	10 μL/reaction

Table 7: PCR parameters for DNA amplification using FirePol® DNA polymerase

PCR Step	Temperature	Duration	Cycles
Initialization	95°C	1 min	
Denaturation	95°C	30 sec	35X
Annealing	42°C	40 sec	
Elongation	62°C	1min/1kbp	
Final elongation	62°C	1 min	
Final hold	4°C	forever	

3.1.6 Plasmid DNA isolation from *E. coli* strains (Mini-prep)

The positive clones from the PCR screen (Section 3.1.5) was grown in 5 mL of liquid LB media with the appropriate selection drug overnight at 37°C, shaking. 500 μL of overnight culture was resuspended in glycerol stabilate, and stored at -80°C as a reservoir.

The remaining overnight culture was harvested via centrifugation, and the plasmid DNA was extracted using the NucleoSpin®Plasmid kits (Macherey Nagel). The final purified DNA was sent for sequencing or stored at -20°C.

3.1.7 Sequencing of plasmid DNA

For each sequencing reaction, 5 µL of DNA (concentration of 100 ng/µL) and 5 µL of primer (concentration of 1 µM) was prepared and sent to MOBIX Lab. The primers used for sequencing can be found in Section 2.8.2.

3.1.8 Plasmid DNA isolation from *E. coli* strains (Midi-prep)

Verified clones containing the plasmid with the correct insert were selected and grown in 200 mL of liquid LB media with the correct selection drug. The cells were harvested and plasmid DNA was extracted using the Plasmid Midi Kit (Qiagen).

The DNA concentration was determined using the NanoDrop 2000, and the final purified DNA was verified to have the correct insert through test digests (refer to Section 3.1.3). Validated samples were then prepared for transfection into *P. falciparum* 3D7 parental cell line (Section 3.1.9), or stored at -20°C.

3.1.9 DNA precipitation and preparation for transfection

For transfecting the plasmid DNA into *P. falciparum* 3D7 parental cell line, the appropriate volume of the DNA resulting from the midi-prep for 100 µg of DNA was calculated for precipitation. 10 % of the calculated sample volume of 3 M NaAc and 3 times the sample volume of 100 % EtOH was added and briefly vortexed. The sample was then stored at -20°C for at least one hour.

The sample was then centrifuged at full speed for 20 min. The supernatant was discarded and the pellet was washed once with 500 µL of 70 % EtOH. The tube was kept closed and transferred to a BSL-2 safety cabinet. The supernatant was then removed and the pellet was dried until translucent. The DNA pellet was then resuspended with 15 µL of pre-warmed sterile TE buffer. Next steps are described in Section 3.3.4.

3.2 Microbiological experiments

3.2.1 Cultivation of *E. coli* strains

E. coli was either grown on LB agar plates or liquid LB media with the appropriate selection drug (ampicillin or kanamycin).

For *E. coli* cultivation on LB plates, *E. coli* cells were resuspended and plated on a LB plate using glass beads. The plate was then incubated at 37°C overnight and stored at 4°C the next day.

For *E. coli* cultivation in liquid LB media, a single bacterial colony was inoculated in 10 mL of LB liquid media with the appropriate selection drug. 500 μL of the overnight culture was resuspended in 500 μL of glycerol stabilate and stored at -80°C as reservoir. The remaining liquid culture was then used for downstream applications.

3.2.2 Preparation of chemically competent *E. coli* cells

Chemo-competent cells were prepared to increase the uptake of plasmid DNA. For both *E. coli* strains used in this thesis, this was done through the rubidium chloride method (Hanahan, 1983), which destabilizes the cell wall of the bacterial cells. Firstly, a single colony of the *E. coli* strain was inoculated with 2 mL of LB media and was grown overnight at 37°C shaking. The next day, the 2 mL overnight culture was transferred to a 1 L Erlenmeyer flask filled with 200 mL of LB media. The 200 mL culture was incubated at 37°C shaking until the OD_{600} was 0.5-0.6. The culture was centrifuged at 2400 x g at 4°C for 20 min. The resulting pellet was resuspended in TFBI buffer and incubated on ice for 10 min. The cells were then centrifuged at 2400 x g for 20 min at 4°C, and the pellet was resuspended in TFBII buffer. The bacteria was divided into 100 μL aliquots in 1.5 mL Eppendorf tubes, snap-frozen in liquid nitrogen, and then stored at -80°C.

3.2.3 Transformation of *E. coli* competent cells with plasmid DNA

The ligation reaction was mixed with thawed competent *E. coli* cell aliquots (100 μL) and incubated on ice for 10 minutes. The cells were then heat shocked at 42°C for 40 sec, and then transferred onto ice for 2 minutes. 650 μL of 1X LB without ampicillin was added to the cells, which were then incubated at 37°C shaking at 900 rpm for 30 min. The cells were then centrifuged for 2 min at 6000 rpm, 650 μL of the supernatant was removed, and the residual supernatant was used to resuspend the bacterial cells, which was then plated on LB plates containing the appropriate drug using glass beads. The plated cells were then incubated at 37°C overnight and stored at 4°C.

All constructs were transformed into *E. coli* XL10-Gold cells. Only the pET28a_GAP45-HIS construct was later transformed into *E. coli* BL21 (DE3) cells for overexpression steps (refer to Section 3.2.4).

3.2.4 Protein overexpression in *E. coli* BL21 (DE3) cells

The correct colony containing the pET28a plasmid with the correct GAP45 insert was grown in 5 mL of liquid LB media with kanamycin overnight at 37°C, shaking. For a small scale overexpression, 50 mL of liquid LB media with kanamycin was inoculated with the overnight culture (1:100 dilution) in a 1 L Erlenmeyer flask. The 50 mL culture was then grown at 37°C, shaking until OD_{600} reached 0.4-0.6. A 1 mL sample of the uninduced culture was reserved before adding IPTG to a final concentration of 1 mM, which induces protein overexpression. The culture was induced for 3-4 hours, and then a 1 mL sample of the induced culture was collected before harvesting the cells by

centrifuging at 4000 x g for 20 min at 4°C. The supernatant was removed and the resulting pellet was stored at -20°C for further purification steps (Section 3.4.5).

The collected uninduced and induced samples were prepared for SDS-PAGE analysis to ensure proper induction.

For large scale overexpression, 50 mL of overnight culture was grown instead, 300 mL of culture per 1 L Erlenmeyer flask was prepared.

3.2.5 Bacterial cell lysis via homogenization

Bacteria pellets harvested from a 2 L culture as described in Section 3.2.4 were resuspended in 50 mL of lysis buffer. DNaseI (NEB) was added to a final concentration of 5 U/mL, and mixed for 30 min at 4°C. The suspension was homogenized using the Emulsiflex C3 (ATA Scientific) under the following conditions: 4 passes under a constant pressure of 15,000 psi at 4°C. The consistency of the final emulsion was water-like, which is then centrifuged at 4000 rpm for 30 min at 4°C. 20 μL of the supernatant or lysate was reserved and prepared for SDS-PAGE analysis. The remainder of the lysate material can be stored at -20°C, or was used to proceed in Section 3.4.4.1.

3.3 Cell biological experiments

3.3.1 Continuous culture of *P. falciparum*

Plasmodium falciparum parasites were grown using the protocol established by Trager and Jensen, 1976. The parasites were grown in 5 mL (15 x 60 mm) or 10 mL (14 x 90 mm) Petri dishes. The growth conditions were at 37°C under an environment of 5 % O_2, 5 % CO_2, and 90 % N_2, in RPMI with 5 % hematocrit. Depending on the transgenic cell line, either the selective agent 1.5 μg/mL of Blasticidin or 10 nM of WR99210 was used. To maintain parasite cultures, the parasitemia of the culture was determined according to the Giemsa stained blood smears (Section 3.3.2), which was kept under 10% through appropriate dilutions.

3.3.2 Giemsa stained blood smears

To determine the parasitemia of a culture, 1.5 μL of erythrocytes was retrieved from the bottom of the culture dish, placed onto a glass slide, and smeared by another glass slide to achieve a monolayer of cells. The smear was then air dried, fixed in 100 % methanol, which was then stained in 10 % Giemsa stain for a minimum of 15 min. The blood smear was then rinsed with tap water, briefly dried with paper towel, and then visualized using a standard light microscope (Zeiss). Parasitemia can be calculated by the following equation:

[infected red blood cells (iRBC)/ red blood cells (RBC)] x 100 %

3.3.3 Synchronization of *P. falciparum* (Lambros & Vanderberg, 1979)

To maintain parasites within a parasite culture to be within the same time frame of the intraerythrocytic cycle, culture containing mixed blood stages are synchronized to eliminate all parasite stages that are not rings. To synchronize the parasites, 5 or 10 mL cultures were centrifuged at 1500 x g for 5 min. The supernatant was removed, and the erythrocyte pellet was resuspended with 4 times the volume synchronization solution. The suspension was incubated at 37°C for 10 min, and then centrifuged at 1500 x g for 5 min. The supernatant was discarded, and the remaining erythrocyte pellet was resuspended with 5 mL or 10 mL (depending on the volume of the starting culture material) RPMI, and blood was added accordingly to achieve 5 % hematocrit. The synchronization solution, which contains 5 % D-Sorbitol, eliminates all blood stages except for ring stage parasites due to hypotonic pressure. The resulting culture should only have ring stage parasites within the 0-16 hours post invasion time frame.

3.3.4 Transfection of plasmid DNA into *P. falciparum* 3D7 (Wu et al., 1995)

The resuspended DNA pellet described in Section 3.1.9 was resuspended in 385 μL of pre-warmed Cytomix. 250 μL of erythrocytes from a synchronized ring stage *P. falciparum* 3D7 culture with a parasitemia of <5% was mixed with the DNA/Cytomix sample, and transferred to a 2 mm electroporation cuvette (Bio-Rad), and electroporated using a Gene Pulser Xcell (Bio-Rad) at 0.310 kV and 950 μF. The sample was then immediately transferred to a 10 mL petri dish with 4% erythrocytes in 10 mL pre-warmed RPMI medium. After 4 hours, the media was exchanged and the selection drug was added. The medium was changed once everyday for the next 10 days, and then every other day. Normally, parasites are visible 4-6 weeks post transfection in Giemsa stained blood smears.

3.3.5 Storage of parasites

3.3.5.1 Freezing of parasite stabilates

10 mL or 5 mL of synchronous ring stage parasite culture with a parasitemia of >5 % was centrifuged at 1500 x g for 5 min. The supernatant was discarded and the remaining pellet was resuspended with two times the volume of malaria freezing solution (MFS). The suspension was transferred into a CryoTube and stored in liquid nitrogen.

3.3.5.2 Thawing of parasites

A CryoTube of frozen parasite culture was thawed in a 37°C water bath. The thawed parasites were transferred into a 15 mL falcon tube and centrifuged at 1500 x g for 5 min. The supernatant was discarded and the pellet was resuspended in 1 mL of pre-warmed malaria thawing solution (MTS). The suspension was centrifuged at 1500 x g for 5 min. The supernatant was discarded, and the remaining pellet was resuspended with 5 mL or 10 mL (depending on the volume of the frozen culture) of pre-warmed RPMI, and erythrocytes were added to achieve 5 % hematocrit.

3.3.6 Parasite isolation through saponin lysis (Umlas and Fallon, 1971)

10 mL of parasite culture was centrifuged at 1500 x g for 5 min. The supernatant was discarded and the erythrocyte pellet was resuspended with 1 mL of saponin lysis buffer, and the suspension was transferred to a 2 mL Eppendorf tube. The suspension was filled up to a final volume of 2 mL using saponin lysis buffer, mixed by inversion, and then incubated on ice for 10 min. The suspension was then centrifuged at full speed for 5 min. The pellet was rinsed with 1 mL 1 X PBS three times. The final pellet can be stored dry at -20°C, or the can be used for protein extraction steps (Section 3.4.1).

3.4 Biochemical experiments

3.4.1 Protein extraction from sample pellet

The sample pellet was resuspended in 30-100 μL of dH_2O depending on the pellet size, and the appropriate volume of 5 X SDS sample buffer was added. The sample was vortexed, and then cooked at 95°C for 10 min. The cooked sample was then centrifuged for 5 min at full speed. The supernatant was then loaded onto a SDS-PAGE gel or stored at -20°C.

3.4.2 SDS-PAGE (Sodium Dodecyl Sulfate Polyacrylamide Gel Electrophoresis) (Schagger & von Jagow,1987)

SDS-PAGE using a discontinuous system was used to separate proteins by their molecular weight. The purpose of a discontinuous system is to concentrate the sample before the separation of the protein occurs. This system utilizes two types of gels- the stacking gel and the separating gel, which are 4 % and 10 % polyacrylamide gels, and at pH 6.8 and 8.8 respectively. The gels are prepared according to Section 2.4.4.1. The proteins are separating via an electric current, with more negative proteins travelling further down the gel towards the cathode. The SDS-PAGE was conducted at 200 V for 1 hour.

3.4.3 Western blot analysis

Proteins were transferred onto a nitrocellulose membrane using the wet-transfer system using the 1 X wet transfer buffer (Bio-Rad). All Whatman paper, nitrocellulose membrane, SDS-PAGE gel, and foam sponges were pre-soaked in cold 1 X wet transfer buffer, and the apparatus was assembled according to the manufacturer's protocol (Bio-Rad). The proteins were transferred at 100 V for 1 hour per gel.

The membrane was then blocked with blocking solution for 1 hour at room temperature.

The blocking solution was discarded, and the membrane was probed with the appropriate primary antibody (Section 2.7.1) overnight at room temperature.

The primary antibody was removed the next day and stored at -20°C. The membrane was washed three times with wash buffer (1 X PBS with Tween® 20) before incubated with the secondary antibody (Section 2.7.2) for one hour at room temperature. The secondary

antibody was then discarded, and the membrane was washed five times with wash buffer. 1:1 ratio of the Luminol/Enhancer and the Stable Peroxide Buffer provided in the Western Blot ECL-Detection Kit (Thermo Fisher Scientific) was prepared and used to incubate the washed membrane for 5 min in the dark. Excess liquid was removed off the membrane and the membrane was developed on the ChemiDoc™ XRS+ System with Image Lab™(Bio-Rad).

3.4.4 Coomassie staining

Coomassie staining was used to visualize separated proteins on a SDS-PAGE gel. In this thesis, it was specifically used to analyze the level of protein overexpression in *E. coli* BL21 (DE3) (Section 3.2.4). After protein separation (Section 3.4.2), the SDS-PAGE gel was incubated in Coomassie solution for 15 min. The gel was then destained in dH_2O overnight and imaged using the ChemiDoc™ XRS+ System with Image Lab™(Bio-Rad).

3.4.5 Protein purification

3.4.5.1 Ni-NTA purification (gravity-flow column method)

To purify the His-tagged fusion protein, 4 mL of Ni-NTA slurry (2 mL bed volume) was added to an Econo-Pac® Chromatography Column (Bio-Rad). The NI-NTA resin was washed with water twice, and the beads were equilibrated twice with five times the bed volume of buffer A.

The column was capped, and the lysate obtained from Section 3.2.5 was incubated with the resin for 30 min at 4°C, rotating.

The column was then uncapped, and the flowthrough was collected.

10 mL of buffer A was added to the column, and the fraction was collected as wash 1. To eliminate unspecific binding and contaminants, 10 mL of the wash buffer, which contains a high salt concentration, was added to the column (wash 2). 10 mL of buffer A was added to the column once again to remove the high salt content (wash 3).

The HIS-tagged protein was eluted in two steps with different imidazole concentrations. The last elution step was to ensure that all HIS-tagged proteins were eluted from the NI-NTA resin. First, 15 mL of 200 mM imidazole containing buffer was added to the column (elution 1). After, 5 mL of buffer B was added to the column (elution 2). 20µL of all collected fractions were reserved and prepared for SDS-PAGE analysis.

3.4.5.2 Dialysis

To remove any small macromolecules and contaminants in the elution fractions obtained from Section 3.4.5.1, which may interfere with latter purification steps, all elution fractions were pooled and dialyzed. A 2 L beaker with a magnetic stirrer was filled with the prepared 1 L of dialysis buffer. The elution fractions were added together in a dialysis sack with a pore size of 12 kDa Molecular Weight Cut-Off (MWCO) (Sigma-Aldrich),

which ensures that any protein larger than 12 kDa will not diffuse out of the semi-permeable dialysis sack. The dialysis was conducted overnight at 4°c, stirring.

3.4.5.3 Protein concentration

The dialyzed elution fractions were concentrated before being injected into the ÄKTA FPLC system for latter gel filtration procedures. The protein was concentrated using a Corning® Spin-X® UF concentrators Spin-X UF 6; 10 kDa MWCO (Sigma-Aldrich) until the final volume was 1 mL.

3.4.5.4 Gel filtration using the ÄKTA system

To further purify the HIS-tagged protein after Ni-NTA purification, gel filtration was conducted to remove contaminants according to size. This method utilizes a column containing a dextran and agarose matrix using fast liquid chromatography (FPLC). Smaller molecules will interact and diffuse in the matrix, and there be eluted later in the purification process. On the other hand, larger molecular weight molecules will be eluted from the column first due to the lack of interaction with the matrix. In this thesis, Superdex 200 10/300 GL (GE Healthcare) was used with the ÄKTA system.

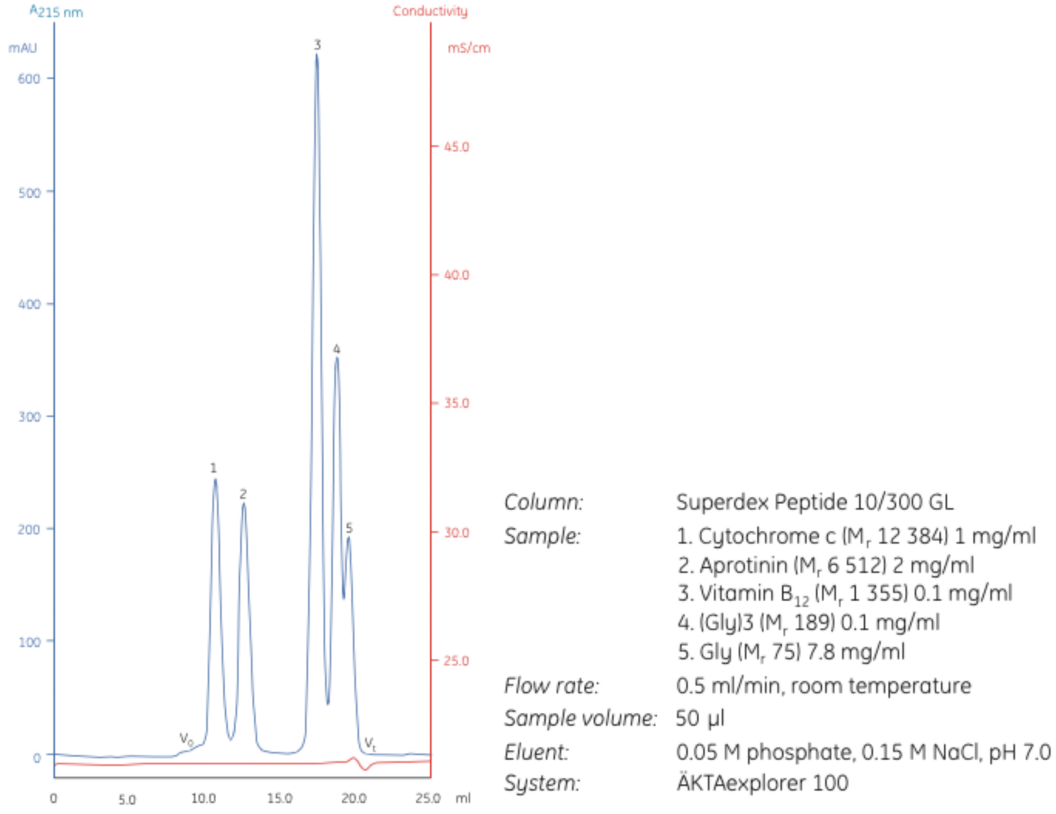

Figure 8. Standard peptide separation using the Superdex Peptide 10/300 GL (GE Healthcare, 2007).

Gel filtration buffer was used to equilibrate the column, and the concentrated protein (Section 3.4.5.3) was injected. The fractions were collected in 1 mL fractions in a 96-well plate. Fractions with corresponding peaks on the chromatogram were prepared for SDS-PAGE analysis.

3.4.5.5 Protein preparation for crystallization

Samples from Section 3.4.5.4 containing the purified protein was concentrated to 1 mL using Corning® Spin-X® UF concentrators Spin-X UF 6; 10 kDa MWCO (Sigma-Aldrich). The concentrated samples were sent to Hampton Research, EMBL/DESY, Hamburg, Germany for crystallization screens using Crystal Screen 1 and 2. The screens were based on the hanging drop method, with 1 µL of reservoir solution and 1 µL of protein sample. Optimized conditions have not yet been determined.

3.4.6 Solubility assay

Parasites from a 10 mL culture with a parasitemia of 5-10 % was harvested according to Section 3.3.6, and the resulting pellet was resuspended in 100 µL dH_2O and snap-frozen in liquid nitrogen 4 times. The suspension was passed through a 27G needle five times and centrifuged at full speed for 5 min. The supernatant was reserved as the soluble fraction as the previous procedure disrupted the parasite membrane, releasing soluble proteins into the supernatant. The remaining pellet was washed with 500 µL dH_2O two times, and then once with 500 µL 1 X PBS. The pellet was resuspended with 100 µL carbonate buffer for 30 min on ice. The carbonate buffer disrupts protein-protein interactions, hence releasing peripheral membrane proteins into the supernatant. The suspension was centrifuged at full speed for 5 min, and the supernatant was reserved as the peripheral membrane fraction. The remaining pellet was washed three times with 100 µL 1 X PBS, and then resuspended in 100 µL ice cold 0.1 % Triton-X-100/PBS for 30 min on ice. The detergent solubilizes the phospholipid bilayer of membranes, hence releasing integral membrane proteins. The suspension was centrifuged at full speed for 5 min, and the supernatant reserved is integral membrane protein fraction. The pellet was washed with 1 X PBS and resuspended in 100 µL PBS, yielding in the pellet fraction. All fractions were prepared for SDS-PAGE and subsequent Western-blot analysis.

3.4.7 Proteinase K protection assay (Cabrera et al., 2012)

In this thesis, Proteinase K assay was conducted using the GAP50-GFP overexpressing cell line to determine the orientation of GAP50- whether the C-terminal tail of GAP50 is exposed to the cytosol. Saponin lysed parasites were used as starting material as saponin lyses the erythrocyte by permeabilizing the erythrocyte membrane. This exposes the parasite's plasma membrane (PPM), which is then lysed using digitonin. Digitonin is a weak non-ionic detergent, and can permeabilize the plasma membrane without disrupting organelle membranes when used at low concentrations. This is due to the higher cholesterol composition of organelle membranes. Therefore integral membrane proteins will be protected from digitonin (Adam et al., 1990).

To conduct the assay, saponin lysed parasites (Section 3.3.6) from one 10 mL culture with a parasitemia of 5-10 % was used as the starting material. The pellet was resuspended in 1.5 mL of ice cold SoTE, which was divided into three 0.5 mL aliquots. 0.5 mL of cold SoTE was added to tube 1 (control), while 0.5 mL of 0.02 % Digitonin was added to tubes 2 and 3. All samples were inverted and incubated on ice for 10 min, and then centrifuged at 800 x g for 10 min at 4°C. All supernatant was discarded, and 0.5 mL of SoTE was added to tubes 1 and 2, while 0.5 mL of Proteinase K/SoTE was added to tube 3. All sampled were inverted and incubated on ice for 30 min. Cold trichloroacetic acid (TCA) was added to all samples to a final concentration of 10 %, which inactivates Proteinase K activity. All tubes were centrifuged at maximum speed for 20 min, washed with acetone, and then dried. The pellets were resuspended in TE and prepared for SDS-PAGE and subsequent Western-blot analysis.

3.5 Microscopic methods

3.5.1 Light microscopy

The Giemsa stained blood smears (Sections 3.3.2) were analyzed using a light microscope (Zeiss) at 1000 X magnification with immersion oil.

3.5.2 Fluorescence microscopy

3.5.2.1 Live cell microscopy

Live cell microscopy was conducted to analyze transgenic parasites expressed mCherry or green fluorescent protein (GFP) tagged proteins. The 256 amino acid mCherry reporter protein is a derived from the red fluorescent protein isolated from *Discosoma* sp. (Shaner et al., 2004), while GFP was first isolated from the *Aequorea victoria* jellyfish, and is comprised of 238 amino acids (Prasher et al, 1992). In preparation of cells for live cell microscopy, 1 μg/mL of DAPI was added to 400 μL of resuspended parasite culture with a parasitemia of ~5% and incubated at 37°C for 10 min. The sample was centrifuged for 1500 rpm for 30 sec, and the supernatant was partially removed for supernatant and erythrocyte pellet was 1:1 ratio. 8 μL of the resuspended sample was added on a glass slide and covered with a cover slip.

Images were taken using a Zeiss Axioscope M1 with a 100 X oil immersion objective with a Hamamatsu Orca C4742-95 camera. Axio Vision 40 V 4.7.0.0 software was used to collect the pictures.

3.5.2.2 Immunofluorescence assay (IFA)

A 10 mL parasite culture with a parasitemia of approximately 3-5 % was centrifuged at 1500 x g for 5 min. The parasites were fixed by resuspending the erythrocyte pellet with 1 mL of formaldehyde/glutaraldehyde fixation solution. The suspension was incubated at room temperature for 30 min. The fixation was centrifuged at 3000-4000 rpm for 2 min, and the pellet was washed three times with 1 X PBS. After discarding the supernatant, the

membrane was permeabilized with 0.1 % Triton-X-100/PBS for 10 min. The suspension was centrifuged at 6000 rpm for 2 min, and the pellet was washed once with 1 X PBS. The pellet was blocked with 3 % BSA/ 1 X PBS for 1 hour at room temperature, rolling. The blocking solution was removed after centrifugation, and the pellet was incubated with 500 μL of primary antibody dilution (Section 2.7.1) overnight at 4°C. The primary antibody was reserved for later use, and the pellet was washed three times with 1 X PBS. The pellet was incubated with 500 μL of secondary antibody (Section 2.7.2) for 1 hour at room temperature. 1 μg/mL DAPI was added to the incubation for 10 min. The pellet was centrifuged and the supernatant was discarded. The final pellet was resuspended in 50 μL 1 X PBS, and prepared for microscopy using the Zeiss Axioscope M1.

4. Results

4.1 GAP45 is recruited to the inner membrane complex (IMC)

GAP45 (Gene ID: PFL1090w) is comprised of 204 amino acids, and is heavily modified with lipidation and phosphorylation motifs (Figure 1A). GAP45 has a N-terminal dual acylation motif, consisting of a myristoylation site (Rees-Channer et al., 2006) at G2 (NMT prediction score= 1.908; Maurer-Stroh et al., 2002), and a palmitoylation site at C5 (CSS-Palm prediction score= 35.96; Ren et al., 2008). The protein is also shown to be palmitoylated at C160 (Jones et al., 2012), and is has four cysteine residues at the C-terminus (C176, C178, C189, and C192), which may be potential palmitoylation sites. The protein also has eight *in vivo* phosphroylation sites: S89, S103, S107, S142, S149, S156, T158, and S198 (Treeck et al., 2011). Altogether, these protein modifications may be responsible for GAP45 recruitment to the IMC, where the episomally expressed GAP45-mCherry protein is localized to the IMC (Figure 9B1, 13B2). The solubility profile of GAP45-mCherry also agrees with the IMC phenotype, where the protein is fractionated as a peripheral membrane protein (Figure 9B3). IMC localization of GAP45 is further validated through immunofluorescence assay (IFA) using the IMC marker GAPM2 (Kono et al., 2012) (Figure 9C).

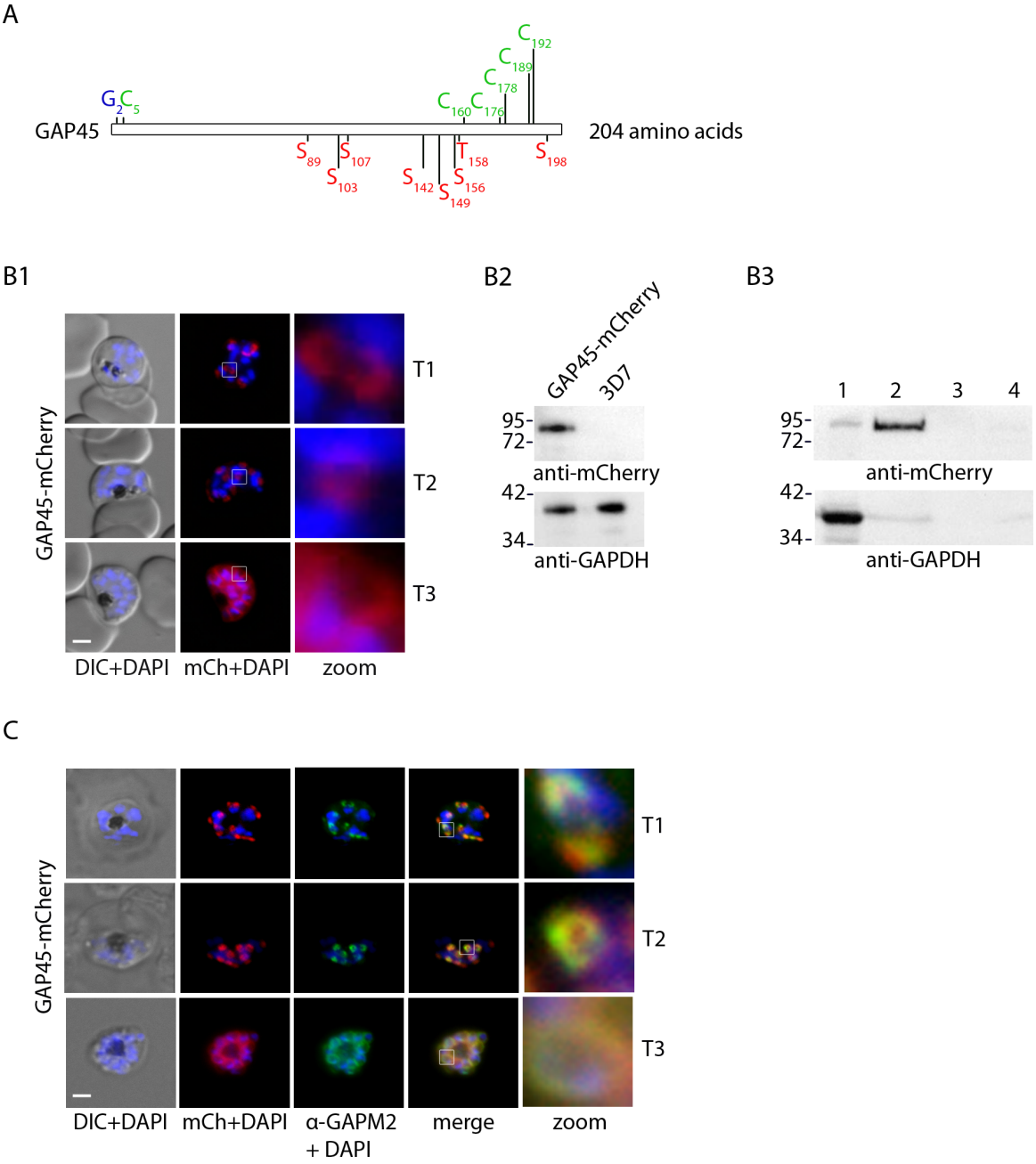

Figure 9. Schematic representation of GAP45 with lipidation and phosphorylation modifications and its localization during schizogony. (A) GAP45 is predicted to be myristoylated (blue) and palmitoylated (green). The protein is also heavily phosphorylated *in vivo* (red). (B1) The overexpression of GAP45-mCherry is exhibits an IMC phenotype, visualizing IMC biogenesis during cell division. This involves three steps: T1 (cramp-like structures), T2 (ring-like structures), and T3 (IMC is underlying the plasma membrane of each nascent merozoite). Nuclei are stained with DAPI. (B2) Expression of GAP45-mCherry is analyzed through Western blot using anti-mCherry antibodies. (B3) The solubility of the GAP45-mCherry protein was analyzed using solubility assay. The resulting fractions are 1) hypotonic 2) carbonate soluble 3) 1% Triton-X-100

soluble and 4) insoluble fractions. GAP45-mCherry is mainly present in the carbonate soluble fraction- evidence that it localized to the IMC as a peripheral membrane protein. (C) Co-localization of GAP45-mCherry with α-GAPM2 using IFA confirms the IMC localization of GAP45. Scale bar, 2 μm.

4.2 Dissection of lipidation motifs in IMC recruitment of GAP45

4.2.1 The N-terminus is a secondary determinant for IMC localization

To decipher the mode of GAP45 recruitment to the IMC in terms of lipidation motifs, the protein was dissected into two parts- the N-terminus containing the dual acylation motif, and the C-terminus containing the 5 cysteine residues. As the N-terminus has been previously shown to re-localize the protein to the plasma membrane instead of the IMC (Cabrera et al., 2012; Ridzuan et al., 2012), a GAP45 construct with a deletion of the first 29 amino acids ($_{\Delta 29}$GAP45-mCherry) was generated (Figure 10A). The mutant could not be recruited to any membrane, and was localized to the cytosol (Figure 10B1, 10B2). This phenotype was validated via a solubility assay, where $_{\Delta 29}$GAP45-mCherry was only found in the hypotonic fraction, a solubility profile corresponding to soluble and hence cytosolic proteins (Figure 10B3). Altogether, these results provide evidence that the C-terminus is insufficient in proper IMC localization of GAP45, and also requires the N-terminus for proper recruitment to the IMC.

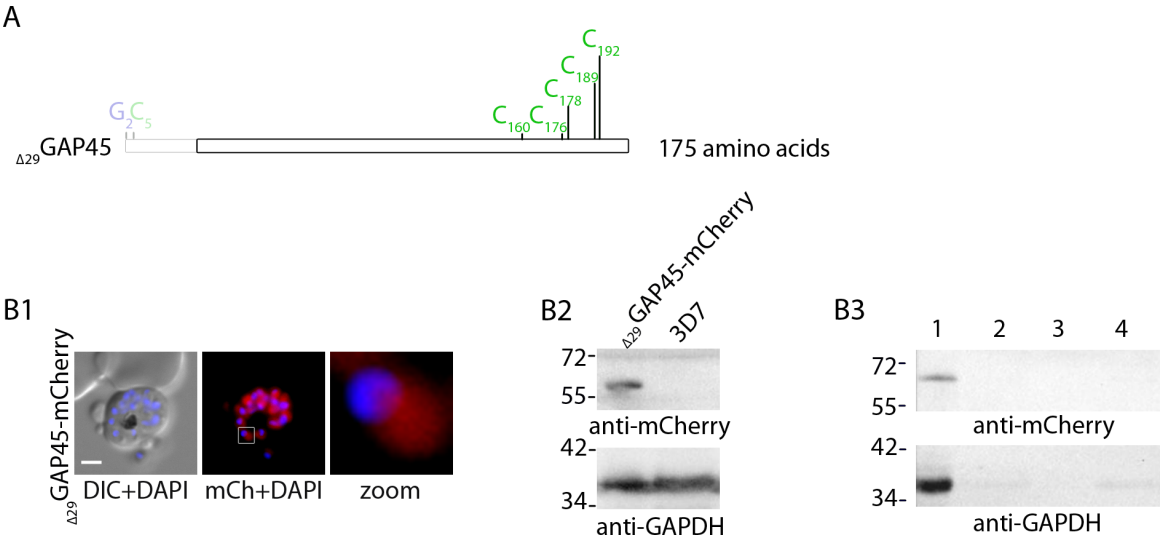

Figure 10. N-terminal deletion of GAP45 leads to a cytosolic variant. (A) The deletion of the first 29 amino acids ($_{\Delta 29}$GAP45-mCherry) leads to a (B1) cytosolic variant. (B2) the expression of $_{\Delta 29}$GAP45-mCherry was analyzed via Western blot. (C) The solubility assay showed that the $_{\Delta 29}$GAP45-mCherry mutant was only present in the hypotonic fraction, representative of a cytosolic protein. Scale bar, 2 μm.

4.2.2 C189 and C192 are essential in IMC recruitment

In order to determine whether palmitoylation at the C-terminus is the mode of IMC recruitment of GAP45, all five C-terminal predicted and putative palmitoylation sites were abolished through alanine substitution, resulting in a palmitoylation null mutant ($GAP45_{palmnull}$-mCherry) (Figure 11A). $GAP45_{palmnull}$-mCherry was recruited to the plasma membrane instead of the IMC (Figure 11B1, 11B2). This observation was further validated through IFA using the IMC marker GAPM2 (Figure 11C). Therefore palmitoylation at one or more of the C-terminal residues is critical for GAP45 association to the IMC.

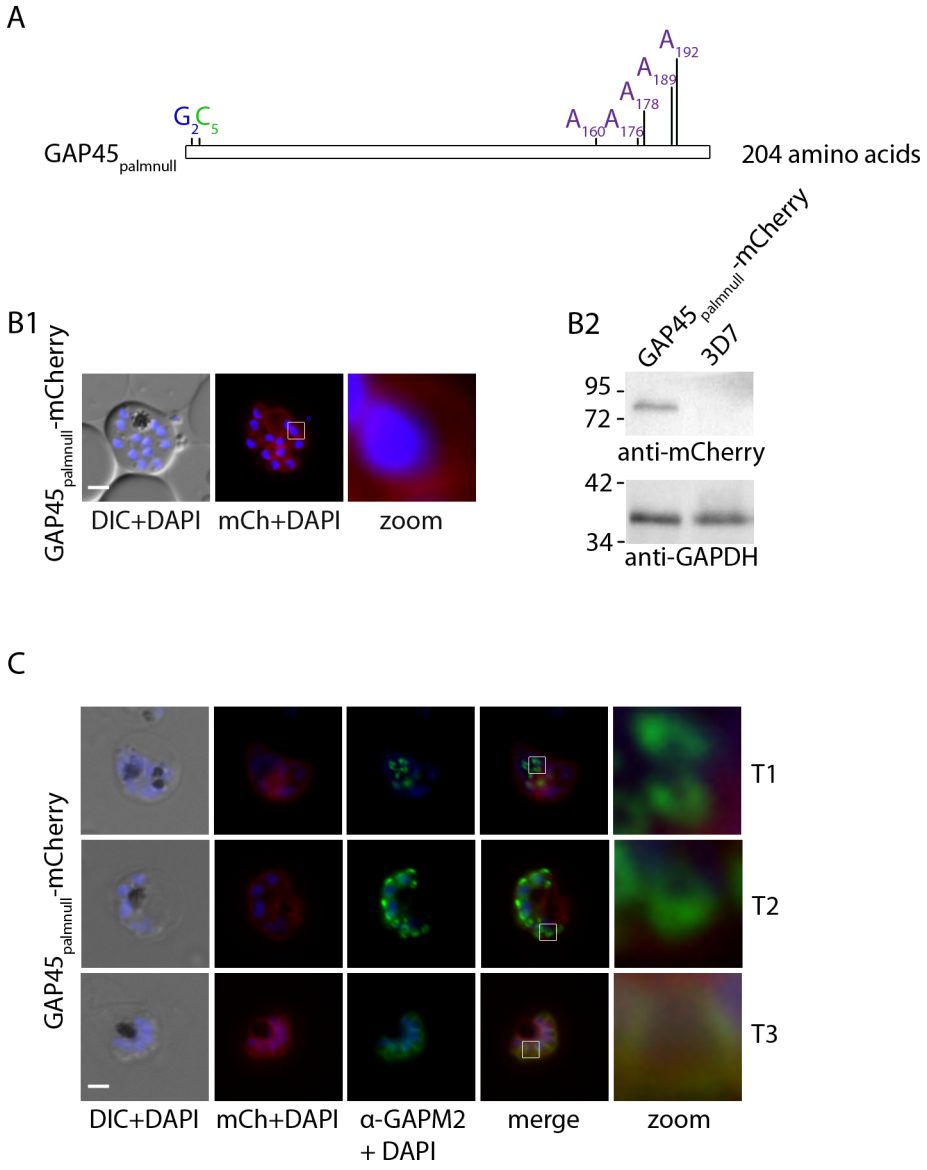

Figure 11. Removal of C-terminal putative palmitoylation sites lead re-distribution of GAP45 to the plasma membrane. (A) The C-terminal putative palmitoylation sites were mutated into

alanines (purple), while keeping the N-terminal myristoylation (blue) and palmitoylation sites (green) intact. The construct was fused to a C-terminal mCherry protein, resulting in a palmitoylation null mutant ($GAP45_{palmnull}$-mCherry). (B1) $GAP45_{palmnull}$-mCherry is localized to the plasma membrane and (B2) its expression is analyzed via Western blot. (C) The plasma membrane localization of the mutant was validated through IFA with the IMC marker GAPM2 (green). Scale bar, 2 μm.

To pinpoint the exact C-terminal putative palmitoylation sites responsible for IMC recruitment, the lipidation sites were individually abolished via alanine substitution and fused to a C-terminal mCherry protein, yielding in the constructs $GAP45_{C160A}$-mCherry, $GAP45_{C176AC178A}$-mCherry, $GAP45_{C178A}$-mCherry, $GAP45_{C189A}$-mCherry, and $GAP45_{C192A}$-mCherry. It was observed that the mutations C160A, C176A, and C178A had no effect on IMC localization (Figure 12A-C). However, the mutations C189A (Figure 13A) and C192A (Figure 13B) led to a plasma membrane phenotype, which were validated via IFA and a double transgenic cell line respectively (Figure 13A3, 13B3, 13B4). Therefore, the residues C189 and C192 are essential in recruiting GAP45 to the IMC.

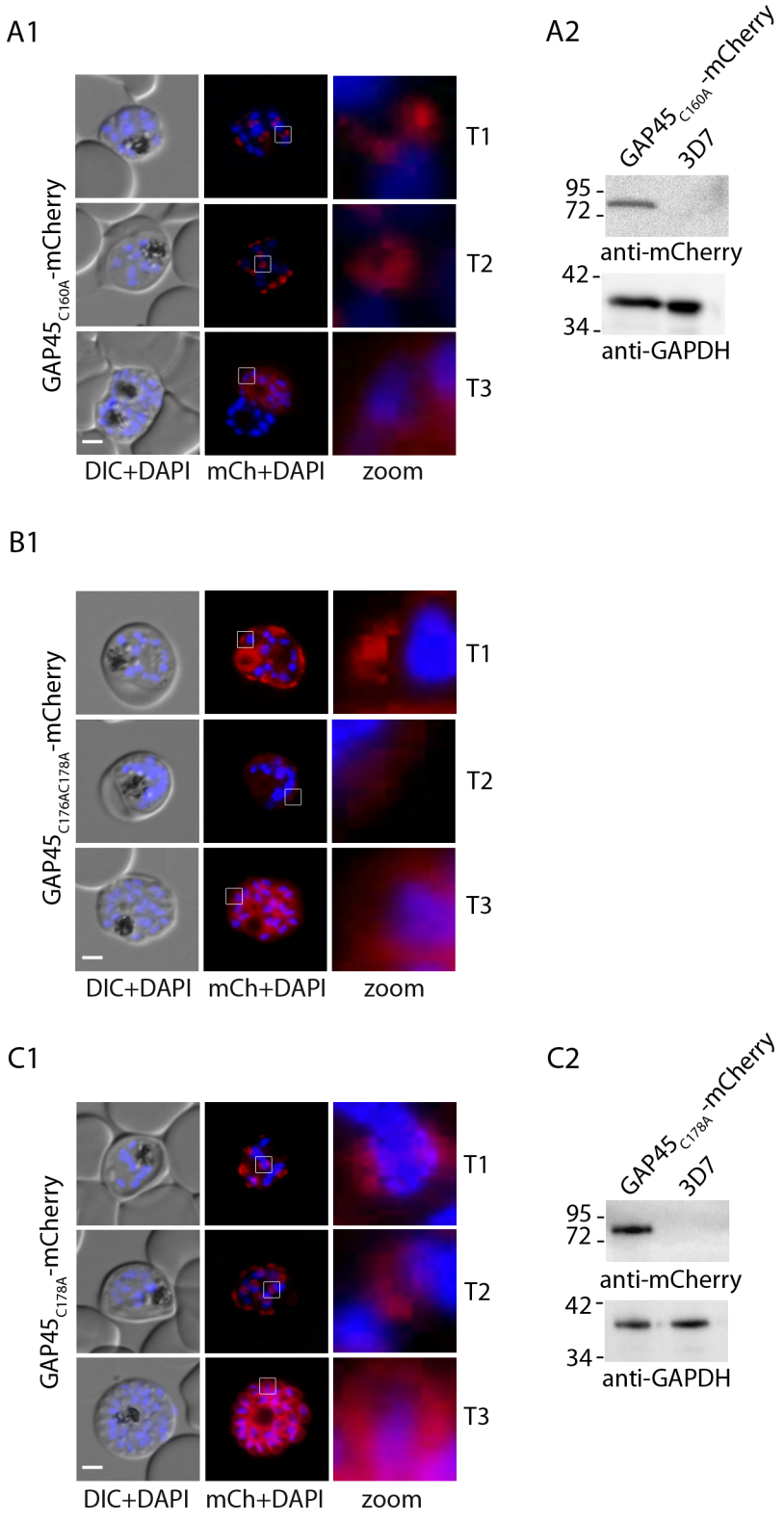
A1
A2
GAP45C160A-mCherry
T1
T2
T3
DIC+DAPI
mCh+DAPI
zoom
GAP45C160A-mCherry
3D7
95
72
anti-mCherry
42
34
anti-GAPDH
B1
GAP45C176AC178A-mCherry
T1
T2
T3
DIC+DAPI
mCh+DAPI
zoom
C1
C2
GAP45C178A-mCherry
T1
T2
T3
DIC+DAPI
mCh+DAPI
zoom
GAP45C178A-mCherry
3D7
95
72
anti-mCherry
42
34
anti-GAPDH

Figure 12. Overexpression of C160A, C176A/C178A, and C178A mutants shows no change in IMC phenotype. (A1) GAP45$_{C160A}$-mCherry, (B1) GAP45$_{C176AC178A}$-mCherry, and (C1) GAP45$_{C178A}$-mCherry were overexpressed and the resulting phenotypes show no change in GAP45 recruitment to the IMC. (A2, C2) The expression of each transgenic cell line was analyzed through Western blot. Scale bar, 2 μm.

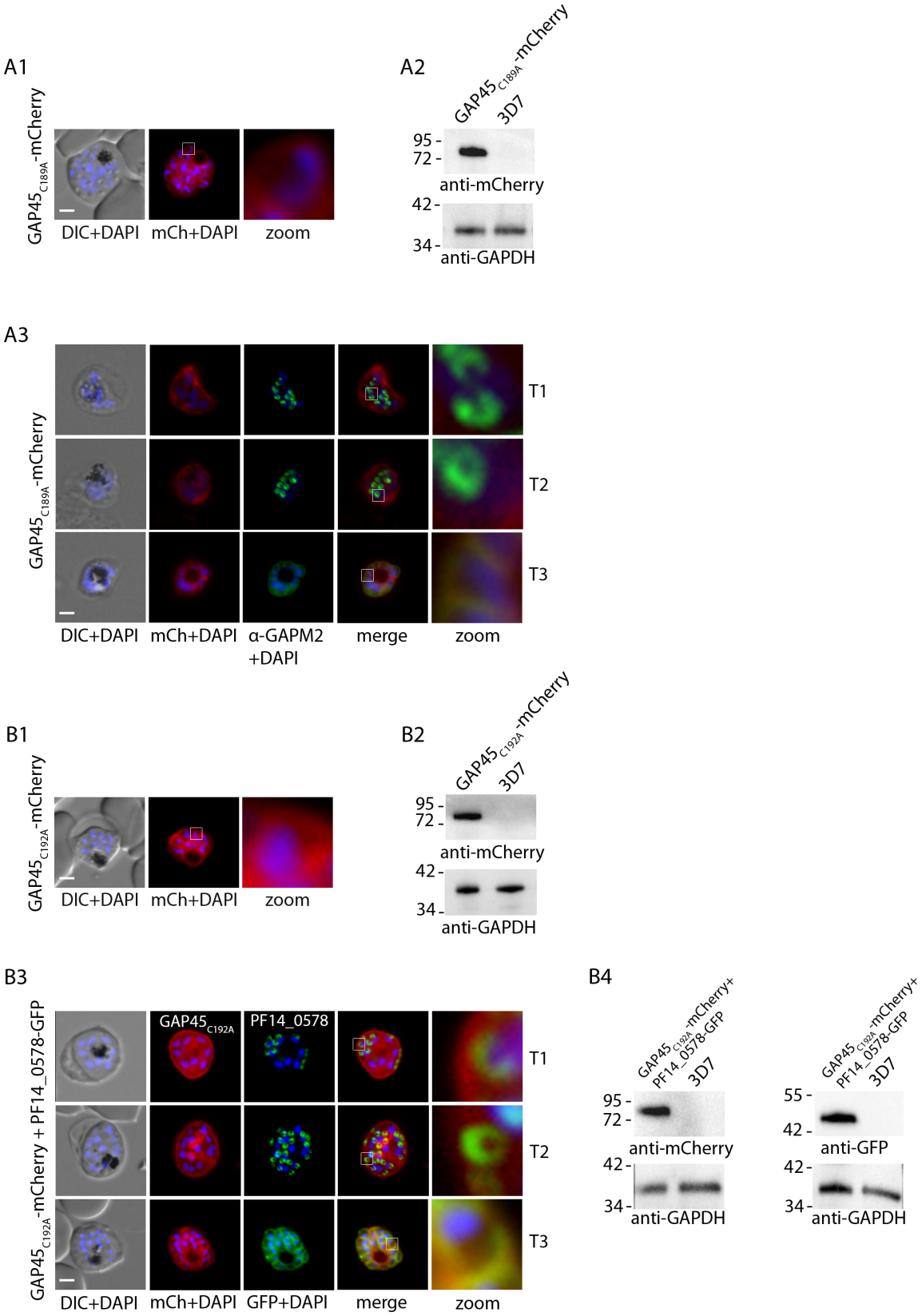
A1
GAP45C189A-mCherry
DIC+DAPI
mCh+DAPI
zoom
A2
GAP45C189A-mCherry
3D7
95 -
72 -
anti-mCherry
42 -
34 -
anti-GAPDH
A3
GAP45C189A-mCherry
T1
T2
T3
DIC+DAPI
mCh+DAPI
α-GAPM2 +DAPI
merge
zoom
B1
GAP45C192A-mCherry
DIC+DAPI
mCh+DAPI
zoom
B2
GAP45C192A-mCherry
3D7
95 -
72 -
anti-mCherry
42 -
34 -
anti-GAPDH
B3
GAP45C192A-mCherry + PF14_0578-GFP
GAP45C192A
PF14_0578
T1
T2
T3
DIC+DAPI
mCh+DAPI
GFP+DAPI
merge
zoom
B4
GAP45C192A-mCherry+ PF14_0578-GFP
3D7
95 -
72 -
anti-mCherry
42 -
34 -
anti-GAPDH
55 -
42 -
anti-GFP
42 -
34 -
anti-GAPDH

Figure 13. C189 and C192 are essential for proper IMC localization of GAP45. (A1) $GAP45_{C189A}$-mCherry was overexpressed, and the mutation exhibited plasma membrane localization. (A2) The expression was analyzed via Western blot. (A3) The plasma membrane phenotype was validated using IFA with the IMC marker GAPM2, where co-localization was only observed in the T3 stages. (B1) The C192A mutation also led to a plasma membrane phenotype, and the (B2) expression of the mutant protein was analyzed through Western blot. (B3) To confirm the plasma membrane phenotype, a double transgenic cell line overexpressing $GAP45_{C192A}$-mCherry and PF14_0578-GFP was generated. $GAP45_{C192A}$-mCherry only co-localized with PF14_0578-GFP in the T3 stages of IMC biogenesis, supporting that the C192A phenotype is indeed plasma membrane. Scale bar, 2 μm.

4.3 IMC recruitment of GAP45 is independent of phosphorylation

Besides lipidation motifs, GAP45 also is abundant with eight *in vivo* phosphorylation sites. To investigate whether phosphorylation plays a role in IMC recruitment of GAP45, all phosphorylation sites were substituted with alanines, resulting in a $GAP45_{phosnull}$-mCherry construct (Figure 14A). When the construct was episomally overexpressed, it was localized to the IMC (Figure 14B1, 14B2). Therefore IMC recruitment of GAP45 is independent of phosphorylation events.

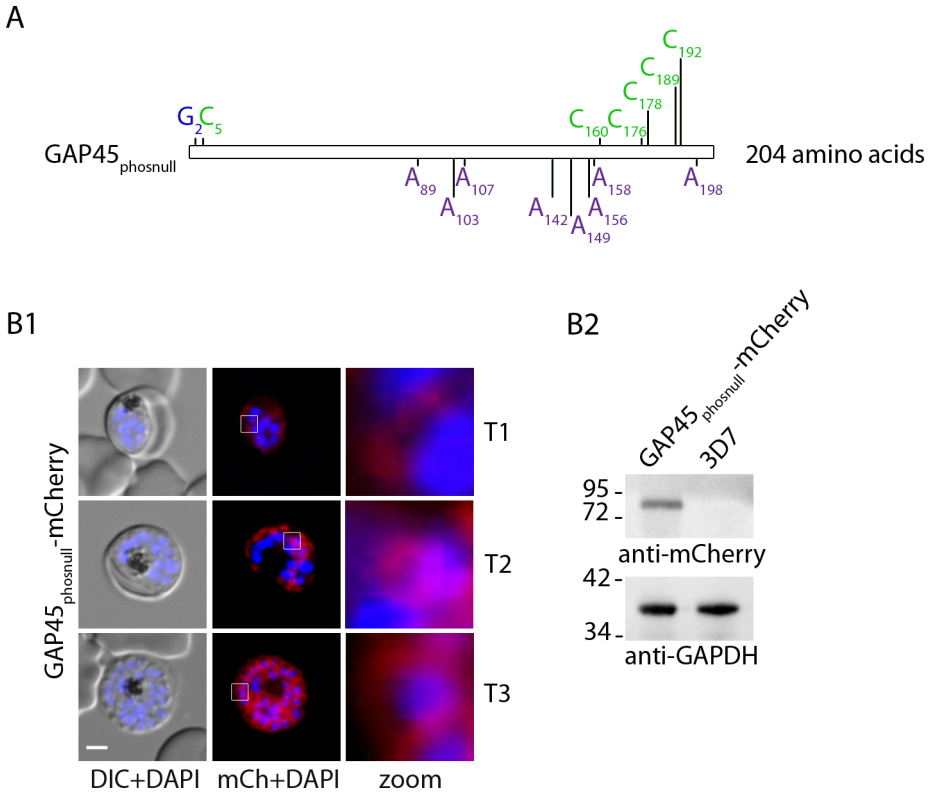

Figure 14. Phosphorylation does not play a role in IMC recruitment of GAP45. (A) All *in vivo* phosphorylation sites were abolished via alanine substitution (purple), which was fused to a C-terminal mCherry reporter, hence creating the $GAP45_{phosnull}$-mCherry construct. (B1) $GAP45_{phosnull}$-

mCherry is localized to the IMC despite the lack of phosphorylation sites. (B2) The expression of $GAP45_{phosnull}$-mCherry was analyzed through Western blot. Scale bar, 2 μm.

4.4 Crystallization of GAP45

To further understand the interaction between GAP45 and other glideosome members such as GAP50, the next step was to gain structural insight of GAP45. GAP45 was cloned into the pET28a vector, generating a C-terminally 6xHIS tagged GAP45 construct (GAP45-HIS). The protein was overexpressed in *E. coli* BL21 (DE3) and purified using Ni-NTA gravity-flow column method and fast protein liquid chromatography (FPLC) in collaboration with Dr. Christian Löw at the EMBL Deutsches Elektronen-Synchrotron (DESY) campus in Hamburg, Germany.

The purification was conducted under two conditions: without any reducing agent, and with the reducing agent tris(2-carboxyethyl)phosphine (TCEP). This reducing agent causes an irreversible reaction, breaking disulfide bonds in a protein (Yoshida et al., 2005). This is particularly important in the case of GAP45 where its C-terminus is rich in cysteine residues, and hence prone to improper intermolecular folding via disulfide bridges.

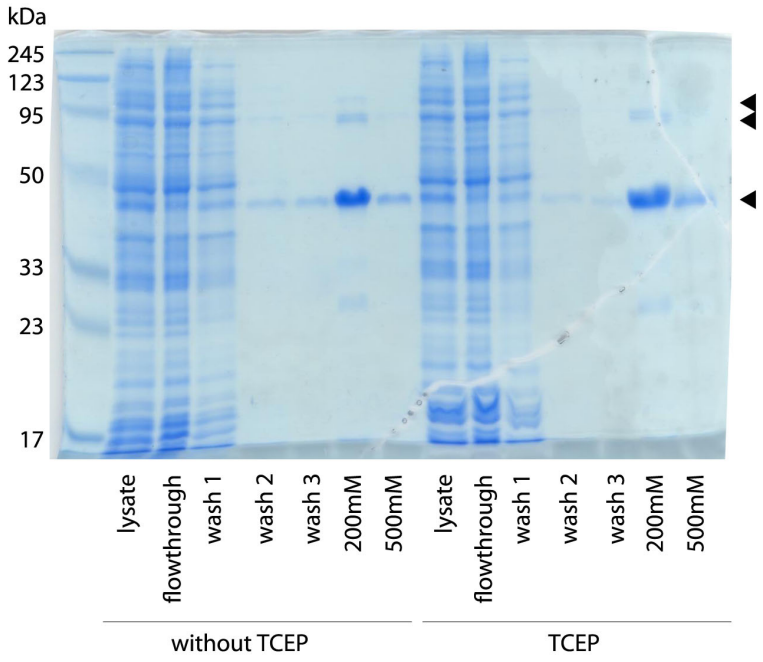

Figure 15. Ni-NTA purification of GAP45-HIS with and without reducing agent. GAP45-HIS was purified through the Ni-NTA gravity-flow column method with and without TCEP, where all collected fractions were visualized using SDS-PAGE stained with Coomassie solution. The lysate represents input sample for the Ni-NTA column, which is the supernatant of the lysed bacterial pellet. After flowthrough, the column was washed three times before being eluted with two imidazole concentrations: 200mM and 500mM. Protein bands of ~46 kDa and higher as indicated by the black arrowheads were observed in the elution fractions under both conditions.

GAP45-HIS was first purified using Ni-NTA gravity-flow column method, where a protein of approximately 46 kDa was extracted from the bacterial lysate under both conditions with or without TCEP (Figure 15). Protein bands of approximately 46 kDa and higher were eluted under both conditions. As the protein species were not homogenous in the elution fractions, they were pooled separately and subjected to gel filtration purification.

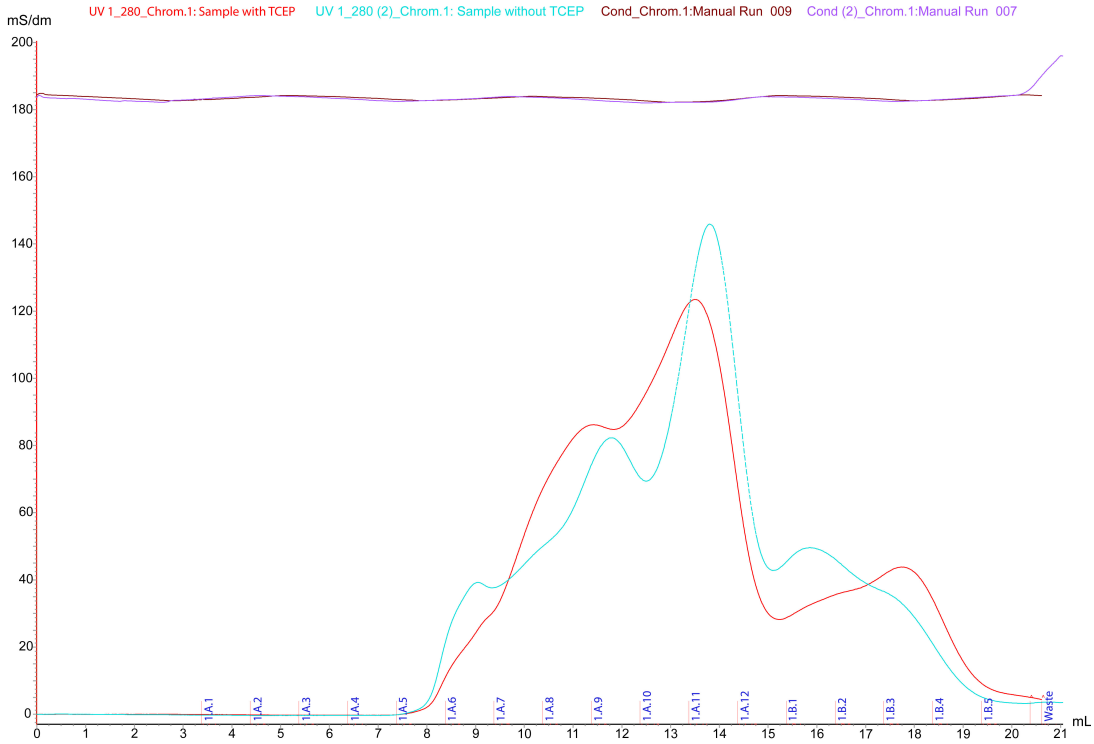

Figure 16. Chromatogram of GAP45-HIS gel filtration purification. The pooled elution fractions from the Ni-NTA purification under no TCEP and with TCEP conditions were purified using gel filtration with the ÄKTA system. The gel filtration purification process was recorded using the UNICORN™ 6.3 software. The red line represents the elution sample with TCEP, and the cyan line represents the elution sample without TCEP. The brown and purple lines show the salt conductivity in the run with TCEP and without TCEP respectively. The blue numbering represents the 1 mL fractions collected during the purification process. The two peaks in each individual run represents a different protein species, and therefore indicating that the GAP45-HIS monomer was unable to be separated from the oligomers.

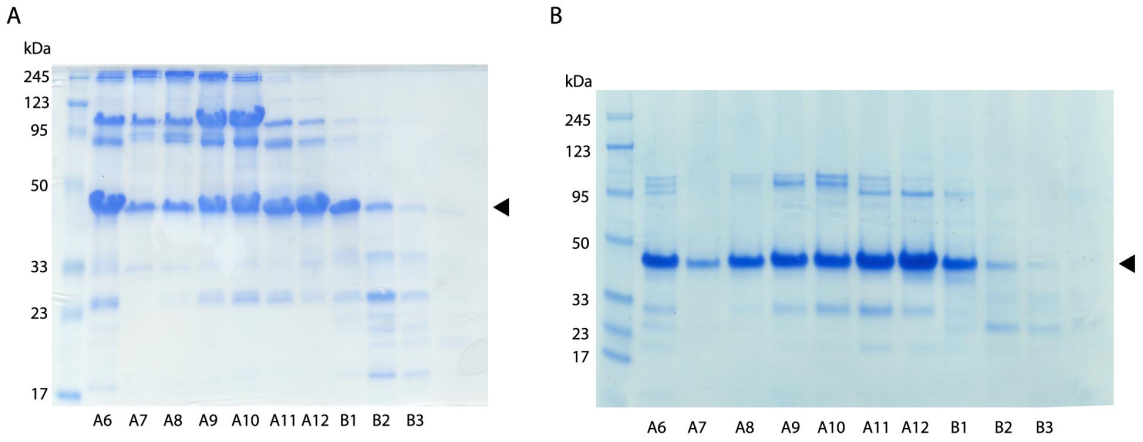

Figure 17. Gel filtration purification of GAP45-HIS. GAP45-HIS collected from the previous purification (A) without TCEP and (B) with TCEP were purified through gel filtration. The fractions A6 to B3 obtained from the gel filtration purification were visualized using Coomassie stained SDS-PAGE gels. It is evident that less oligomers were present under the TCEP preparation, and the target band of ~46 kDa is still present as indicated by the black arrowhead.

The gel filtration purification allowed successful isolation of a more homogenous protein species under the TCEP condition (Figure 17). The protein was further validated to be GAP45-HIS through Western blot which was probed with anti-HIS, as well as mass spectrometry (Löw, unpublished). Mass spectrometry confirmed that the protein is monomeric. All fractions A6-B3 collected under TCEP conditions were pooled and concentrated to 10.3 mg/mL. 1 mL of the protein sample was then sent for a crystallization screen, which resulted in the following micro-crystals (Figure 18). Unfortunately, the crystals were too small in size, thus requiring further optimization in the purification process and crystallization conditions (Benvenuti & Mangani, 2007).

Figure 18. GAP45-HIS crystals. GAP45-HIS micro-crystals as indicated by the black arrows were observed after a week during the crystallization screen. However, the crystals did not continue to grow, hence requiring optimization in both purification steps as well as crystallization conditions for higher quality crystals.

5. Conclusion and Discussion

5.1 IMC recruitment of GAP45 requires the N-terminal dual acylation motif, C189, and C192

In previous work, it was shown that the N-terminal dual acylation motif is insufficient in recruiting GAP45 to the IMC (Cabrera et al., 2012; Ridzuan et al., 2012). However, the C-terminus of GAP45 alone was incapable of any type of membrane association considering that the N-terminal deletion construct ($_{\Delta 29}$GAP45-mCherry) remained localized in the cytosol (Figure 10). Combining these data sets, the N-terminal dual acylation motif as well as the C-terminus of GAP45 are both essential to proper IMC localization. Specifically, the cysteine residues in the C-terminus are a secondary requirement for IMC recruitment of GAP45, as shown by the GAP45$_{palmnull}$-mCherry construct, which remained associated to the plasma membrane (Figure 11).

As one of the C-terminal cysteine residues, C160, was already shown to be palmitoylated through mass spectrometry (Jones et al., 2012a), it is extremely likely that palmitoylation within the C-terminus is a major contributor to the protein's IMC localization, specifically at residues C189 and C192 (Figure 13). These results agree with a study conducted in *T. gondii*, where the conserved C-terminal residues at C230 and C233 were also shown to be essential to the protein's recruitment to the IMC (Frenal et al., 2010). Altogether, these results do suggest that GAP45 bridges the intermembrane space between the plasma membrane and the IMC (Frenal et al., 2010).

5.2 Controversy of GAP45 spanning between the IMC and the PPM

The intermembrane space is hypothesized to be approximately 20-25 nm (Frenal et al., 2010). GAP45 is a 23.6 kDa protein, and assuming that it may take form of a sphere, its calculated minimum diameter is 3.78 nm (Erickson, 2009). Also, based on mass spectrometry data with the purified protein (Figure 17), GAP45 exists as a monomer (Löw, unpublished). Altogether, it is highly unlikely that GAP45 will span the entire intermembrane space. To support this, GAP45 is currently in the progress to be crystallized, where the exact size of the tertiary protein structure will be determined (Gilberger and Löw, unpublished).

Another argument against this model is that the distance must also be shared among other glideosome members, including aldolase which interacts with filamentous (F) actin, MyoA, and MTIP (Baum et al., 2006b) (Figure 5). If GAP45 were to occupy the entire intermembrance space, it may become a physical obstacle interfering with the action of the actin-myosin motor. It is possible that the N-terminal constructs (Cabrera et al., 2012; Ridzuan et al., 2012) are localized to the plasma membrane by default due to the dual acylation motif, and requires the C-terminal residues C189 and C192 for specific membrane targeting to the IMC.

5.3 Interaction between GAP45 and GAP50

The GAP45 structure will not only be important in envisioning the model of the glideosome complex, but it will allow us to speculate possible protein-protein interacting domains of GAP45.

GAP45 contains a coiled- coil domain at approximately residues 14-123 (Combet et al., 2000), where coiled-coil domains typically plays a role in protein-protein interaction (Burkhard et al., 2001). The GAP45 structure may allow one to deduce possible interactions with a glideosome partner and the coiled-coil domain depending on how the domain is exposed after protein folding. Although C189 and C192 are essential for GAP45 recruitment to the IMC, there is no hard evidence supporting that these two residues are key in interacting with GAP50 or with glideosome assembly.

GAP50 is a 44.6 kDa protein, and unlike the other glideosome components, it is co-translationally embedded into the endoplasmic reticulum (ER) of the parasite which is transported to the IMC (Gaskins et al., 2004; Yeoman et al., 2011). GAP50 is comprised of a hydrophobic N-terminal signal peptide, which is cleaved off after protein maturation, an acid phosphatase homology domain, and a C-terminal transmembrane domain followed by a five amino acid tail which is predicted to be cytoplasmic (Gaskins et al., 2004; Yeoman et al., 2011).

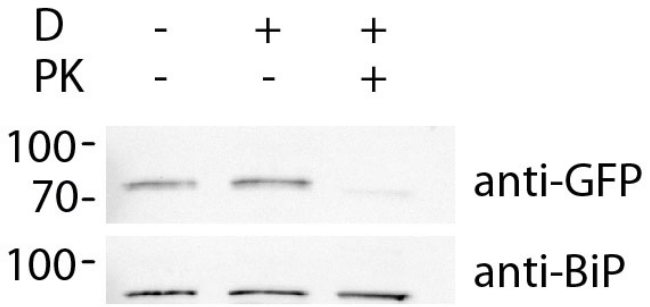

Figure 19. The C-terminal tail of GAP50 is exposed to the cytoplasmic space. Parasite material extracted from a GAP50-GFP overexpressing cell line was used for Proteinase K protection assay, revealing GAP50's topology. The parasite plasma membrane (PPM) was permeabilized using digitonin (D), and Proteinase K (PK) cleaves any protein exposed in the parasite cytoplasm. Anti-BiP (Struck et al., 2005) was used a control to ensure that organelle membranes were not disrupted.

The C-terminal tail of GAP50 was shown to be essential in the interacting with the proto-glideosome, where the *T. gondii* mutant lacking the C-terminal five amino acids was unable to interact with MyoA, MTIP, and GAP45 (Gaskins et al, 2004). A Proteinase K protection assay also confirmed the topology of GAP50 (Figure 19). Using a GAP50-GFP overexpressing cell line, the C-terminal GFP protein was successfully cleaved by Proteinase K, validating that the C-terminus is not protected by the IMC organelle. To ensure that organelle membranes were not disrupted by digitonin, hence still protecting

integral membrane proteins from Proteinase K activity, BiP was used as a control. BiP is the 72 kDa immuno-globulin binding protein, which resides within the lumen of the endoplasmic reticulum (ER) (Kumar et al., 1988).

To further study the exact mode of interaction between GAP45 and GAP50, a peptide interaction assay would be conducted. Currently, this project has been outsourced to the Löw lab, where the peptide GASSFLSKNMK (C-terminal 11 amino acids) will be used for the peptide-protein interaction study; a longer peptide was chosen due to a higher stability than the five amino acid peptide. GAP50 peptide-GAP45 protein complexes can then be isolated by rapid gel filtration, allowing the mode of interaction to be analyzed (Flynn et al., 1991).

5.4 Role of phosphorylation of GAP45

Although GAP45 is heavily phosphorylated (Treeck et al., 2010), IMC recruitment of GAP45 is independent of phosphorylation events (Figure 14). In this thesis, only threonine and serine phosphorylation sites were investigated, as there are no tyrosine kinases in the *Plasmodium* genus (Ward et al., 2004; Solyakov et al., 2011). However, a recent phosphoproteome study of all intraerythrocytic stages showed that tyrosine phosphorylation accounts for 4.5% of all phosphorylated residues (Pease et al., 2013). Tyrosine phosphorylation also peaks during schizogony compared to ring and trophozoite stages in the intraerythrocytic cycle (Pease et al., 2013), and kinases with dual-specificity such as *Pf*nek3 have been described (Low et al., 2012). Therefore it is possible that potential tyrosine phosphorylation sites were neglected in this thesis work.

Also, assuming that phosphorylation truly does not have an effect in IMC recruitment, one should not exclude the possibility of phosphorylation playing a role in glideosome assembly. As lipidation motifs play a role in membrane association, it is possible that GAP45 is recruited to the IMC membrane via myristoylation and palmitoylation, where phosphorylation initiates association of the proto-glideosome with GAP50 or other glideosome associated proteins.

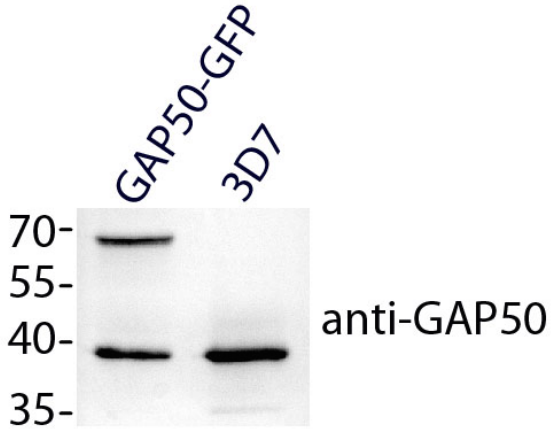

Figure 20. The GAP50 antibody detects GAP50-GFP as well as the endogenous GAP50 protein.

The role of GAP45 phosphorylation can be further investigated through co-immunoprecipitation studies. With the two existing cell lines GAP45-mCherry and $GAP45_{phosnull}$-mCherry, co-immunoprecipitation can be performed using the GAP50 antibody (Figure 20) (Jones et al., 2006). If phosphorylation is indeed required for the interaction between GAP45 and GAP50, then GAP50 should only be detected in the immunoprecipitation of GAP45-mCherry, but not in the phosphoryaltion null mutant.

Another tool to study whether phosphorylation plays a role in glideosome assembly is to generate the double transgenic cell lines GAP45-mCherry/GAP40-GFP and $GAP45_{phosnull}$-mCherry/GAP40-GFP.

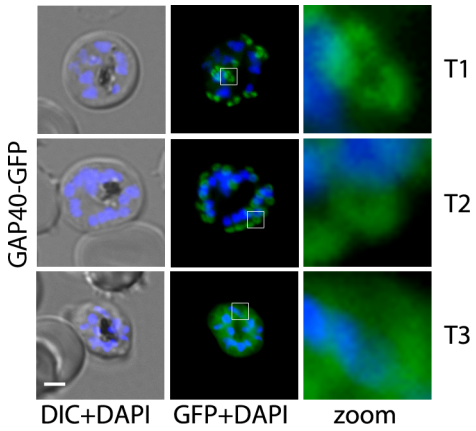

Figure 21. Live cell imaging of the GAP40-GFP overexpressing cell line. GAP40-GFP exhibits the traditional IMC phenotype during the T1, T2, and T3 stages. The nuclei are stained with DAPI. Scale bar, 2 μm.

GAP40 is a 37 kDa protein containing 10 transmembrane domains and is localized to the IMC (Figure 21). GAP40 is also associated with the glideosome complex (Frenal et al., 2010). To date, there is no hard evidence supporting that GAP45 is directly interacting with GAP50; considering that GAP40 is embedded within the IMC with its transmembrane domains, it could be the anchor of glideosome complex to the IMC instead of GAP50. However, the topology of GAP40 must be determined, which could be achieved through Proteinase K protection assay in the same manner as Figure 19 with a cell line overexpressing GAP40 fused to a C-terminal GFP tag. Altogether, this data will allow us to understand i) whether phosphorylation of GAP45 plays a role in glideosome assembly and ii) the role of GAP40 in the glideosome. Understanding the role of another glideosome member is important, as it will expand our knowledge of the invasion process, critical in pinpointing potential drug targets against the malaria parasite.

6. References

Adam, S. A., Marr, R. S., & Gerace, L. (1990). Nuclear protein import in permeabilized mammalian cells requires soluble cytoplasmic factors. *J Cell Biol, 111*(3), 807-816.

Aikawa, M., Miller, L. H., Johnson, J., & Rabbege, J. (1978). Erythrocyte entry by malarial parasites. A moving junction between erythrocyte and parasite. *J Cell Biol, 77*(1), 72-82.

Anamika, Srinivasan, N., & Krupa, A. (2005). A genomic perspective of protein kinases in Plasmodium falciparum. *Proteins, 58*(1), 180-189. doi: 10.1002/prot.20278

Barnes, D. A., Foote, S. J., Galatis, D., Kemp, D. J., & Cowman, A. F. (1992). Selection for high-level chloroquine resistance results in deamplification of the pfmdr1 gene and increased sensitivity to mefloquine in Plasmodium falciparum. *EMBO J, 11*(8), 3067-3075.

Baruch, D. I., Gormely, J. A., Ma, C., Howard, R. J., & Pasloske, B. L. (1996). Plasmodium falciparum erythrocyte membrane protein 1 is a parasitized erythrocyte receptor for adherence to CD36, thrombospondin, and intercellular adhesion molecule 1. *Proc Natl Acad Sci U S A, 93*(8), 3497-3502.

Baum, J., Papenfuss, A. T., Baum, B., Speed, T. P., & Cowman, A. F. (2006a). Regulation of apicomplexan actin-based motility. *Nat Rev Microbiol, 4*(8), 621-628. doi: 10.1038/nrmicro1465

Baum, J., Richard, D., Healer, J., Rug, M., Krnajski, Z., Gilberger, T. W., . . . Cowman, A. F. (2006b). A conserved molecular motor drives cell invasion and gliding motility across malaria life cycle stages and other apicomplexan parasites. *J Biol Chem, 281*(8), 5197-5208. doi: 10.1074/jbc.M509807200

Benvenuti, M., & Mangani, S. (2007). Crystallization of soluble proteins in vapor diffusion for x-ray crystallography. *Nat Protoc, 2*(7), 1633-1651. doi: 10.1038/nprot.2007.198

Bosch, J., Paige, M. H., Vaidya, A. B., Bergman, L. W., & Hol, W. G. (2012). Crystal structure of GAP50, the anchor of the invasion machinery in the inner membrane complex of Plasmodium falciparum. *J Struct Biol, 178*(1), 61-73. doi: 10.1016/j.jsb.2012.02.009

Bosch, J., Turley, S., Roach, C. M., Daly, T. M., Bergman, L. W., & Hol, W. G. (2007). The closed MTIP-myosin A-tail complex from the malaria parasite invasion machinery. *J Mol Biol, 372*(1), 77-88. doi: 10.1016/j.jmb.2007.06.016

Boucher, L. E., & Bosch, J. (2015). The apicomplexan glideosome and adhesins - Structures and function. *J Struct Biol*. doi: 10.1016/j.jsb.2015.02.008

Bousema, T., & Drakeley, C. (2011). Epidemiology and infectivity of Plasmodium falciparum and Plasmodium vivax gametocytes in relation to malaria control and elimination. *Clin Microbiol Rev, 24*(2), 377-410. doi: 10.1128/CMR.00051-10

Bouwman, H., van den Berg, H., & Kylin, H. (2011). DDT and malaria prevention: addressing the paradox. *Environ Health Perspect, 119*(6), 744-747. doi: 10.1289/ehp.1002127

Bullen, H. E., Tonkin, C. J., O'Donnell, R. A., Tham, W. H., Papenfuss, A. T., Gould, S., . . . Gilson, P. R. (2009). A novel family of Apicomplexan glideosome-associated proteins with an inner membrane-anchoring role. *J Biol Chem, 284*(37), 25353-25363. doi: 10.1074/jbc.M109.036772

Burkhard, P., Stetefeld, J., & Strelkov, S. V. (2001). Coiled coils: a highly versatile protein folding motif. *Trends Cell Biol, 11*(2), 82-88.

Butler, A. R., Khan, S., & Ferguson, E. (2010). A brief history of malaria chemotherapy. *J R Coll Physicians Edinb, 40*(2), 172-177.

Bzik, D. J., Li, W. B., Horii, T., & Inselburg, J. (1987). Molecular cloning and sequence analysis of the Plasmodium falciparum dihydrofolate reductase-thymidylate synthase gene. *Proc Natl Acad Sci U S A, 84*(23), 8360-8364.

Cabrera, A., Herrmann, S., Warszta, D., Santos, J. M., John Peter, A. T., Kono, M., . . . Gilberger, T. W. (2012). Dissection of minimal sequence requirements for rhoptry membrane targeting in the malaria parasite. *Traffic, 13*(10), 1335-1350. doi: 10.1111/j.1600-0854.2012.01394.x

Cao, J., Kaneko, O., Thongkukiatkul, A., Tachibana, M., Otsuki, H., Gao, Q., . . . Torii, M. (2009). Rhoptry neck protein RON2 forms a complex with microneme protein AMA1 in Plasmodium falciparum merozoites. *Parasitol Int, 58*(1), 29-35. doi: 10.1016/j.parint.2008.09.005

Cavalier-Smith, T. (1993). Kingdom protozoa and its 18 phyla. *Microbiol Rev, 57*(4), 953-994.

Chalfie, M. (1995). Green fluorescent protein. *Photochem Photobiol, 62*(4), 651-656.

Chulay, J. D., Watkins, W. M., & Sixsmith, D. G. (1984). Synergistic antimalarial activity of pyrimethamine and sulfadoxine against Plasmodium falciparum in

vitro. *Am J Trop Med Hyg, 33*(3), 325-330.

Combet C., Blanchet C., Geourjon C. & Deléage G. (2000) NPS@: Network Protein Sequence Analysis. TIBS 2000 March Vol. 25, No 3 [291]:147-150

Cowman, A. F., Berry, D., & Baum, J. (2012). The cellular and molecular basis for malaria parasite invasion of the human red blood cell. *J Cell Biol, 198*(6), 961-971. doi: 10.1083/jcb.201206112

Douse, C. H., Green, J. L., Salgado, P. S., Simpson, P. J., Thomas, J. C., Langsley, G., . . . Cota, E. (2012). Regulation of the Plasmodium motor complex: phosphorylation of myosin A tail-interacting protein (MTIP) loosens its grip on MyoA. *J Biol Chem, 287*(44), 36968-36977. doi: 10.1074/jbc.M112.379842

Douse, C.H., Mass, S.J., Thomas, J.C., Garnett, J.A., Cota, E., Tate, E.W. (2013) Structural examination of constrained Plasmodium falciparum myosin A peptide helices using pentenyl glycine stapling and hydrogen bond surrogate approaches. *Protein Data Bank.* http://dx.doi.org/10.2210/pdb4mzk/pdb.

Egan, T. J. (2008). Haemozoin formation. *Mol Biochem Parasitol, 157*(2), 127-136. doi: 10.1016/j.molbiopara.2007.11.005

Erickson, H. P. (2009). Size and shape of protein molecules at the nanometer level determined by sedimentation, gel filtration, and electron microscopy. *Biol Proced Online, 11*, 32-51. doi: 10.1007/s12575-009-9008-x

Farrow, R. E., Green, J., Katsimitsoulia, Z., Taylor, W. R., Holder, A. A., & Molloy, J. E. (2011). The mechanism of erythrocyte invasion by the malarial parasite, Plasmodium falciparum. *Semin Cell Dev Biol, 22*(9), 953-960. doi: 10.1016/j.semcdb.2011.09.022

Fitch, C. D. (2004). Ferriprotoporphyrin IX, phospholipids, and the antimalarial actions of quinoline drugs. *Life Sci, 74*(16), 1957-1972. doi: 10.1016/j.lfs.2003.10.003

Florens, L., Washburn, M. P., Raine, J. D., Anthony, R. M., Grainger, M., Haynes, J. D., . . . Carucci, D. J. (2002). A proteomic view of the Plasmodium falciparum life cycle. *Nature, 419*(6906), 520-526. doi: 10.1038/nature01107

Flueck C., Bartfai R., Niederwieser I, Witmer K., Alako B., Moes S., Bozdech Z., Jenoe P., Stunnenberg H., Voss T. 2010. A major role for the Plasmodium falciparum ApiAP2 protein PfSIP2 in chromosome end biology. *PLoS Pathog.* 6:21000784.

Flynn, G. C., Pohl, J., Flocco, M. T., & Rothman, J. E. (1991). Peptide-binding specificity of the molecular chaperone BiP. *Nature, 353*(6346), 726-730. doi:

10.1038/353726a0

Frenal, K., Polonais, V., Marq, J. B., Stratmann, R., Limenitakis, J., & Soldati-Favre, D. (2010). Functional dissection of the apicomplexan glideosome molecular architecture. *Cell Host Microbe, 8*(4), 343-357. doi: 10.1016/j.chom.2010.09.002

Gaji, R. Y., Checkley, L., Reese, M. L., Ferdig, M. T., & Arrizabalaga, G. (2014). Expression of the essential Kinase PfCDPK1 from Plasmodium falciparum in Toxoplasma gondii facilitates the discovery of novel antimalarial drugs. *Antimicrob Agents Chemother, 58*(5), 2598-2607. doi: 10.1128/AAC.02261-13

Gardner, M. J., Hall, N., Fung, E., White, O., Berriman, M., Hyman, R. W., . . . Barrell, B. (2002). Genome sequence of the human malaria parasite Plasmodium falciparum. *Nature, 419*(6906), 498-511. doi: 10.1038/nature01097

Gaskins, E., Gilk, S., DeVore, N., Mann, T., Ward, G., & Beckers, C. (2004). Identification of the membrane receptor of a class XIV myosin in Toxoplasma gondii. *J Cell Biol, 165*(3), 383-393. doi: 10.1083/jcb.200311137

GE Healthcare. (June 2007). *Superdex High-performance Columns*. Retrieved from https://www.gelifesciences.com/gehcls_images/GELS/Related%20Content/Files/1314729545976/litdoc18116379_20140915110638.pdf.

Green, J. L., Rees-Channer, R. R., Howell, S. A., Martin, S. R., Knuepfer, E., Taylor, H. M., . . . Holder, A. A. (2008). The motor complex of Plasmodium falciparum: phosphorylation by a calcium-dependent protein kinase. *J Biol Chem, 283*(45), 30980-30989. doi: 10.1074/jbc.M803129200

Hanahan, D. (1983). Studies on transformation of Escherichia coli with plasmids. *J Mol Biol, 166*(4), 557-580.

Herrera, S., Rudin, W., Herrera, M., Clavijo, P., Mancilla, L., de Plata, C., . . . Certa, U. (1993). A conserved region of the MSP-1 surface protein of Plasmodium falciparum contains a recognition sequence for erythrocyte spectrin. *EMBO J, 12*(4), 1607-1614.

Hasugian, A. R., Purba, H. L., Kenangalem, E., Wuwung, R. M., Ebsworth, E. P., Maristela, R., . . . Price, R. N. (2007). Dihydroartemisinin-piperaquine versus artesunate-amodiaquine: superior efficacy and posttreatment prophylaxis against multidrug-resistant Plasmodium falciparum and Plasmodium vivax malaria. *Clin Infect Dis, 44*(8), 1067-1074. doi: 10.1086/512677

Holder, A. A., Blackman, M. J., Burghaus, P. A., Chappel, J. A., Ling, I. T., McCallum-

Deighton, N., & Shai, S. (1992). A malaria merozoite surface protein (MSP1)-structure, processing and function. *Mem Inst Oswaldo Cruz, 87 Suppl 3*, 37-42.

Hu, G., Cabrera, A., Kono, M., Mok, S., Chaal, B. K., Haase, S., . . . Bozdech, Z. (2010). Transcriptional profiling of growth perturbations of the human malaria parasite Plasmodium falciparum. *Nat Biotechnol, 28*(1), 91-98. doi: 10.1038/nbt.1597

Jones, M. L., Collins, M. O., Goulding, D., Choudhary, J. S., & Rayner, J. C. (2012a). Analysis of protein palmitoylation reveals a pervasive role in Plasmodium development and pathogenesis. *Cell Host Microbe, 12*(2), 246-258. doi: 10.1016/j.chom.2012.06.005

Jones, M. L., Cottingham, C., & Rayner, J. C. (2009). Effects of calcium signaling on Plasmodium falciparum erythrocyte invasion and post-translational modification of gliding-associated protein 45 (PfGAP45). *Mol Biochem Parasitol, 168*(1), 55-62. doi: 10.1016/j.molbiopara.2009.06.007

Jones, M. L., Tay, C. L., & Rayner, J. C. (2012b). Getting stuck in: protein palmitoylation in Plasmodium. *Trends Parasitol, 28*(11), 496-503. doi: 10.1016/j.pt.2012.08.009

Kalanon, M., & McFadden, G. I. (2010). Malaria, plasmodium falciparum and its apicoplast. *Biochemical Society Transactions, 38*(3), 775-782. doi:10.1042/BST0380775; 10.1042/BST0380775

Kannan, R., Sahal, D., & Chauhan, V. S. (2002). Heme-artemisinin adducts are crucial mediators of the ability of artemisinin to inhibit heme polymerization. *Chem Biol, 9*(3), 321-332.

Kim, H., Certa, U., Dobeli, H., Jakob, P., & Hol, W. G. (1998). Crystal structure of fructose-1,6-bisphosphate aldolase from the human malaria parasite Plasmodium falciparum. *Biochemistry, 37*(13), 4388-4396. doi: 10.1021/bi972233h

Kiszewski, A., Mellinger, A., Spielman, A., Malaney, P., Sachs, S. E., & Sachs, J. (2004). A global index representing the stability of malaria transmission. *Am J Trop Med Hyg, 70*(5), 486-498.

Kono, M., Herrmann, S., Loughran, N. B., Cabrera, A., Engelberg, K., Lehmann, C., . . . Gilberger, T. W. (2012). Evolution and architecture of the inner membrane complex in asexual and sexual stages of the malaria parasite. *Mol Biol Evol, 29*(9), 2113-2132. doi: 10.1093/molbev/mss081

Kono, M., Prusty, D., Parkinson, J., & Gilberger, T. W. (2013). The apicomplexan inner membrane complex. *Front Biosci (Landmark Ed), 18*, 982-992.

Kumar, N., Syin, C. A., Carter, R., Quakyi, I., & Miller, L. H. (1988). Plasmodium falciparum gene encoding a protein similar to the 78-kDa rat glucose-regulated stress protein. *Proc Natl Acad Sci U S A, 85*(17), 6277-6281.

Lambros, C., & Vanderberg, J. P. (1979). Synchronization of Plasmodium falciparum erythrocytic stages in culture. *J Parasitol, 65*(3), 418-420.

Leech, J. H., Barnwell, J. W., Aikawa, M., Miller, L. H., & Howard, R. J. (1984). Plasmodium falciparum malaria: association of knobs on the surface of infected erythrocytes with a histidine-rich protein and the erythrocyte skeleton. *J Cell Biol, 98*(4), 1256-1264.

Low, H., Chua, C. S., & Sim, T. S. (2012). Plasmodium falciparum possesses a unique dual-specificity serine/threonine and tyrosine kinase, Pfnek3. *Cell Mol Life Sci, 69*(9), 1523-1535. doi: 10.1007/s00018-011-0888-y

Mabaso, M. L., Sharp, B., & Lengeler, C. (2004). Historical review of malarial control in southern African with emphasis on the use of indoor residual house-spraying. *Trop Med Int Health, 9*(8), 846-856. doi: 10.1111/j.1365-3156.2004.01263.x

Maier, A. G., Cooke, B. M., Cowman, A. F., & Tilley, L. (2009). Malaria parasite proteins that remodel the host erythrocyte. *Nat Rev Microbiol, 7*(5), 341-354. doi: 10.1038/nrmicro2110

Mamoun, C. B., Gluzman, I. Y., Goyard, S., Beverley, S. M., & Goldberg, D. E. (1999). A set of independent selectable markers for transfection of the human malaria parasite Plasmodium falciparum. *Proc Natl Acad Sci U S A, 96*(15), 8716-8720.

Mancio-Silva, L., Lopez-Rubio, J. J., Claes, A., & Scherf, A. (2013). Sir2a regulates rDNA transcription and multiplication rate in the human malaria parasite Plasmodium falciparum. *Nat Commun, 4*, 1530. doi: 10.1038/ncomms2539

Masanja, H., de Savigny, D., Smithson, P., Schellenberg, J., John, T., Mbuya, C., . . . Mshinda, H. (2008). Child survival gains in Tanzania: analysis of data from demographic and health surveys. *Lancet, 371*(9620), 1276-1283. doi: 10.1016/S0140-6736(08)60562-0

Maurer-Stroh, S., Eisenhaber, B., & Eisenhaber, F. (2002). N-terminal N-myristoylation of proteins: prediction of substrate proteins from amino acid sequence. *J Mol Biol, 317*(4), 541-557. doi: 10.1006/jmbi.2002.5426

Meshnick, S. R. (2002). Artemisinin: mechanisms of action, resistance and toxicity. *Int J Parasitol, 32*(13), 1655-1660.

Miller, L. H., Ackerman, H. C., Su, X. Z., & Wellems, T. E. (2013). Malaria biology and disease pathogenesis: Insights for new treatments. *Nature Medicine, 19*(2), 156-167. doi:10.1038/nm.3073; 10.1038/nm.3073

Morrissette, N. S., & Sibley, L. D. (2002). Cytoskeleton of apicomplexan parasites. *Microbiol Mol Biol Rev, 66*(1), 21-38; table of contents.

Murray, C. J., Rosenfeld, L. C., Lim, S. S., Andrews, K. G., Foreman, K. J., Haring, D., . . . Lopez, A. D. (2012). Global malaria mortality between 1980 and 2010: a systematic analysis. *Lancet, 379*(9814), 413-431. doi: 10.1016/S0140-6736(12)60034-8

Nzila, A. M., Mberu, E. K., Sulo, J., Dayo, H., Winstanley, P. A., Sibley, C. H., & Watkins, W. M. (2000). Towards an understanding of the mechanism of pyrimethamine-sulfadoxine resistance in Plasmodium falciparum: genotyping of dihydrofolate reductase and dihydropteroate synthase of Kenyan parasites. *Antimicrob Agents Chemother, 44*(4), 991-996.

Opitz, C., & Soldati, D. (2002). 'The glideosome': a dynamic complex powering gliding motion and host cell invasion by Toxoplasma gondii. *Mol Microbiol, 45*(3), 597-604.

Pease, B. N., Huttlin, E. L., Jedrychowski, M. P., Talevich, E., Harmon, J., Dillman, T., . . . Chakrabarti, D. (2013). Global analysis of protein expression and phosphorylation of three stages of Plasmodium falciparum intraerythrocytic development. *J Proteome Res, 12*(9), 4028-4045. doi: 10.1021/pr400394g

Perkins, M. E., & Rocco, L. J. (1988). Sialic acid-dependent binding of Plasmodium falciparum merozoite surface antigen, Pf200, to human erythrocytes. *J Immunol, 141*(9), 3190-3196.

Petersen, I., Eastman, R., & Lanzer, M. (2011). Drug-resistant malaria: molecular mechanisms and implications for public health. *FEBS Lett, 585*(11), 1551-1562. doi: 10.1016/j.febslet.2011.04.042

Plowe, C. V., Kublin, J. G., & Doumbo, O. K. (1998). P. falciparum dihydrofolate reductase and dihydropteroate synthase mutations: epidemiology and role in clinical resistance to antifolates. *Drug Resist Updat, 1*(6), 389-396.

Prasher, D. C., Eckenrode, V. K., Ward, W. W., Prendergast, F. G., & Cormier, M. J. (1992). Primary structure of the Aequorea victoria green-fluorescent protein. *Gene, 111*(2), 229-233.

Raghavendra, K., Barik, T. K., Reddy, B. P., Sharma, P., & Dash, A. P. (2011). Malaria vector control: from past to future. *Parasitol Res, 108*(4), 757-779. doi: 10.1007/s00436-010-2232-0

Rees-Channer, R. R., Martin, S. R., Green, J. L., Bowyer, P. W., Grainger, M., Molloy, J. E., & Holder, A. A. (2006). Dual acylation of the 45 kDa gliding-associated protein (GAP45) in Plasmodium falciparum merozoites. *Mol Biochem Parasitol, 149*(1), 113-116. doi: 10.1016/j.molbiopara.2006.04.008

Ren, J., Wen, L., Gao, X., Jin, C., Xue, Y., & Yao, X. (2008). CSS-Palm 2.0: an updated software for palmitoylation sites prediction. *Protein Eng Des Sel, 21*(11), 639-644. doi: 10.1093/protein/gzn039

Ridzuan, M. A., Moon, R. W., Knuepfer, E., Black, S., Holder, A. A., & Green, J. L. (2012). Subcellular location, phosphorylation and assembly into the motor complex of GAP45 during Plasmodium falciparum schizont development. *PLoS One, 7*(3), e33845. doi: 10.1371/journal.pone.0033845

Rosenberg, R., & Rungsiwongse, J. (1991). The number of sporozoites produced by individual malaria oocysts. *Am J Trop Med Hyg, 45*(5), 574-577.

Schagger, H., & von Jagow, G. (1987). Tricine-sodium dodecyl sulfate-polyacrylamide gel electrophoresis for the separation of proteins in the range from 1 to 100 kDa. *Anal Biochem, 166*(2), 368-379.

Shaner, N. C., Campbell, R. E., Steinbach, P. A., Giepmans, B. N., Palmer, A. E., & Tsien, R. Y. (2004). Improved monomeric red, orange and yellow fluorescent proteins derived from Discosoma sp. red fluorescent protein. *Nat Biotechnol, 22*(12), 1567-1572. doi: 10.1038/nbt1037

Sidhu, A. B., Verdier-Pinard, D., & Fidock, D. A. (2002). Chloroquine resistance in Plasmodium falciparum malaria parasites conferred by pfcrt mutations. *Science, 298*(5591), 210-213. doi: 10.1126/science.1074045

Solyakov, L., Halbert, J., Alam, M. M., Semblat, J. P., Dorin-Semblat, D., Reininger, L., . . . Doerig, C. (2011). Global kinomic and phospho-proteomic analyses of the human malaria parasite Plasmodium falciparum. *Nat Commun, 2*, 565. doi: 10.1038/ncomms1558

Srinivasan, P., Beatty, W. L., Diouf, A., Herrera, R., Ambroggio, X., Moch, J. K., . . . Miller, L. H. (2011). Binding of Plasmodium merozoite proteins RON2 and AMA1 triggers commitment to invasion. *Proc Natl Acad Sci U S A, 108*(32), 13275-13280. doi: 10.1073/pnas.1110303108

Struck, N. S., de Souza Dias, S., Langer, C., Marti, M., Pearce, J. A., Cowman, A. F., & Gilberger, T. W. (2005). Re-defining the Golgi complex in Plasmodium falciparum using the novel Golgi marker PfGRASP. *J Cell Sci, 118*(Pt 23), 5603-5613. doi: 10.1242/jcs.02673

Sturm, A., Amino, R., van de Sand, C., Regen, T., Retzlaff, S., Rennenberg, A., . . . Heussler, V. T. (2006). Manipulation of host hepatocytes by the malaria parasite for delivery into liver sinusoids. *Science, 313*(5791), 1287-1290. doi: 10.1126/science.1129720

Sullivan, D. J., Jr., Gluzman, I. Y., Russell, D. G., & Goldberg, D. E. (1996). On the molecular mechanism of chloroquine's antimalarial action. *Proc Natl Acad Sci U S A, 93*(21), 11865-11870.

Trager, W., & Jensen, J. B. (1976). Human malaria parasites in continuous culture. *Science, 193*(4254), 673-675.

Treeck, M., Sanders, J. L., Elias, J. E., & Boothroyd, J. C. (2011). The phosphoproteomes of Plasmodium falciparum and Toxoplasma gondii reveal unusual adaptations within and beyond the parasites' boundaries. *Cell Host Microbe, 10*(4), 410-419. doi: 10.1016/j.chom.2011.09.004

Tren, R., & Roberts, D. (2010). DDT and malaria prevention. *Environ Health Perspect, 118*(1), A14-15; author reply A15-16.

Triglia, T., & Cowman, A. F. (1994). Primary structure and expression of the dihydropteroate synthetase gene of Plasmodium falciparum. *Proc Natl Acad Sci U S A, 91*(15), 7149-7153.

Tun, K. M., Imwong, M., Lwin, K. M., Win, A. A., Hlaing, T. M., Hlaing, T., . . . Woodrow, C. J. (2015). Spread of artemisinin-resistant Plasmodium falciparum in Myanmar: a cross-sectional survey of the K13 molecular marker. *Lancet Infect Dis*. doi: 10.1016/S1473-3099(15)70032-0

Umlas, J., & Fallon, J. N. (1971). New thick-film technique for malaria diagnosis. Use of saponin stromatolytic solution for lysis. *Am J Trop Med Hyg, 20*(4), 527-529.

Vahokoski, J., Bhargav, S. P., Desfosses, A., Andreadaki, M., Kumpula, E. P., Martinez, S. M., . . . Kursula, I. (2014). Structural differences explain diverse functions of Plasmodium actins. *PLoS Pathog, 10*(4), e1004091. doi: 10.1371/journal.ppat.1004091

Vulliez-Le Normand, B., Tonkin, M. L., Lamarque, M. H., Langer, S., Hoos, S., Roques, M., . . . Lebrun, M. (2012). Structural and functional insights into the malaria

parasite moving junction complex. *PLoS Pathogens, 8*(6), e1002755. doi:10.1371/journal.ppat.1002755; 10.1371/journal.ppat.1002755

Waller, D., Krishna, S., Crawley, J., Miller, K., Nosten, F., Chapman, D., . . . et al. (1995). Clinical features and outcome of severe malaria in Gambian children. *Clin Infect Dis, 21*(3), 577-587.

Ward, P., Equinet, L., Packer, J., & Doerig, C. (2004). Protein kinases of the human malaria parasite Plasmodium falciparum: the kinome of a divergent eukaryote. *BMC Genomics, 5*, 79. doi: 10.1186/1471-2164-5-79

Wetzel, J., Herrmann, S., Swapna, L. S., Prusty, D., Peter, A. T., Kono, M., . . . Gilberger, T. W. (2015). The role of palmitoylation for protein recruitment to the inner membrane complex of the malaria parasite. *J Biol Chem, 290*(3), 1712-1728. doi: 10.1074/jbc.M114.598094

World Health Organization (WHO). (2014). *WHO World Malaria Report 2014*. Retrieved from http://www.who.int/malaria/publications/world_malaria_report_2014/wmr-2014-profiles.pdf?ua=1.

Wright, M. H., Clough, B., Rackham, M. D., Rangachari, K., Brannigan, J. A., Grainger, M., . . . Tate, E. W. (2014). Validation of N-myristoyltransferase as an antimalarial drug target using an integrated chemical biology approach. *Nat Chem, 6*(2), 112-121. doi: 10.1038/nchem.1830

Wu, Y., Sifri, C. D., Lei, H. H., Su, X. Z., & Wellems, T. E. (1995). Transfection of Plasmodium falciparum within human red blood cells. *Proc Natl Acad Sci U S A, 92*(4), 973-977.

Yahata, K., Treeck, M., Culleton, R., Gilberger, T. W., & Kaneko, O. (2012). Time-lapse imaging of red blood cell invasion by the rodent malaria parasite Plasmodium yoelii. *PLoS One, 7*(12), e50780. doi: 10.1371/journal.pone.0050780

Yeoman, J. A., Hanssen, E., Maier, A. G., Klonis, N., Maco, B., Baum, J., . . . Tilley, L. (2011). Tracking Glideosome-associated protein 50 reveals the development and organization of the inner membrane complex of Plasmodium falciparum. *Eukaryot Cell, 10*(4), 556-564. doi: 10.1128/EC.00244-10

Yoshida, H., Hensgens, C. M., van der Laan, J. M., Sutherland, J. D., Hart, D. J., & Dijkstra, B. W. (2005). An approach to prevent aggregation during the purification and crystallization of wild type acyl coenzyme A: isopenicillin N acyltransferase from Penicillium chrysogenum. *Protein Expr Purif, 41*(1), 61-67. doi: 10.1016/j.pep.2005.02.007